UNIVERSIDADE
LUSÓFONA

CENTRO UNIVERSITÁRIO DE LISBOA
ESCOLA DE PSICOLOGIA E CIÊNCIAS DA VIDA
MESTRADO EM EMBRIOLOGIA E REPRODUÇÃO HUMANA

EXOSOME ANALYSIS IN CULTURE MEDIUM OF HUMAN BLASTOCYSTS RETRIEVED POST-INVASIVE TROPHECTODERM BIOPSY:

POTENTIAL USE AS BIOMARKERS FOR EMBRYONIC VIABILITY

Dissertação defendida a provas públicas para a obtenção do grau de Mestre em Embriologia e Reprodução Humana, orientada pelo Prof. Doutor Ignácio Santiago Alvarez Miguel e Prof. Doutor Bruno Daniel da Costa Gomes

Mariana Belchior Lourenço, nº a22207716
2024

www.ulusofona.pt

CENTRO UNIVERSITÁRIO DE LISBOA
ESCOLA DE PSICOLOGIA E CIÊNCIAS DA VIDA
MESTRADO EM EMBRIOLOGIA E REPRODUÇÃO HUMANA

EXOSOME ANALYSIS IN CULTURE MEDIUM OF HUMAN BLASTOCYSTS RETRIEVED POST-INVASIVE TROPHECTODERM BIOPSY:

POTENTIAL USE AS BIOMARKERS FOR EMBRYONIC VIABILITY

VERSÃO FINAL

Dissertação defendida em provas públicas na Universidade Lusófona, Centro Universitário de Lisboa no dia 24/07/2024, perante o júri, nomeado pelo Despacho de Nomeação n.º: 879/2024, de 2024, com a seguinte composição:

Presidente: Prof. Doutor Patrícia Carla Coelho Rodrigues
Arguente: Prof. Doutor Miguel Gallardo Molina
Orientador: Prof. Doutor Daniel da Costa Gomes

Este trabalho também foi orientado por Prof. Doutor Ignácio Santiago Alvarez Miguel

Mariana Belchior Lourenço, nº a22207716
2024

"The perception of the unknown is the most enthralling of experiences. The individual who remains unattuned to mystery will traverse life without truly perceiving its essence."

Albert Einstein

Acknowledgements

Primarily, I wish to extend my profound gratitude to my entire family and circle of friends for their unconditional support, affection, and patience throughout this journey. For consistently encouraging me and standing steadfastly by my side, irrespective of my choices.

To the Lusófona University of Humanities and Technologies of Lisbon, I extend my sincere gratitude for the financial backing rendered, which facilitated the execution of the overseas internship and master's dissertation. This opportunity has constituted a cornerstone for both my academic and personal advancement.

To all the professionals at the IERA QuironSalud Badajoz clinic, wherein I conducted my internship, who graciously embraced my presence during the ensuing months, I express my gratitude. I wish to particularly acknowledge the invaluable guidance, knowledge dissemination, and support proffered by all the biologists at the clinic throughout the internship period and in the acquisition of samples for the dissertation. Furthermore, my appreciation extends to the University of Badajoz for their receptiveness to process the collected samples at their facility.

A special acknowledgment is reserved for Professor Santiago Álvarez, my dissertation supervisor, for his benevolence, encouragement, and guidance throughout this scholarly endeavour. His unwavering dedication and support have been instrumental in advancing the trajectory of this project.

My earnest appreciation is extended to Professor Bruno Gomes, my internal dissertation supervisor, for his dedicated support, willingness to clarify queries, and provision of constructive feedback. His mentorship has been indispensable at every juncture of this project.

To Professor Patrícia Rodrigues, Professor Mafalda Rato, and Professor Ignácio Santiago Álvarez, the coordinators and educators of this master's programme, for their unwavering commitment, and to all the faculty members of this master's degree for the dissemination of knowledge and dedication throughout this period of academic training.

Finally, to my colleagues in the master's degree, with whom I share an affinity and enthusiasm for this beautiful area, I extend my gratitude for their support throughout these two years of the master's program.

To all those mentioned and to all who have contributed to this dissertation in some way, my deepest gratitude.

Resumo

A seleção eficaz de embriões é fundamental para melhorar as taxas de gravidez clínica em tratamentos de reprodução assistida (TRA). Apesar dos critérios de seleção convencionais, baseados na morfocinética ou no estado cromossómico, persiste o desafio de garantir uma implantação bem-sucedida, mesmo com embriões euploides de alta-qualidade. A produção de vesículas extracelulares por blastocistos *in vitro* foi associada ao processo de implantação, contudo, nenhum estudo semelhante investigou embriões após biopsia para teste genético pré-implantacional (PGT-A).

Este estudo explora o secretoma embrionário como fonte potencial de biomarcadores não invasivos para identificar embriões de excelência adequados para transferência. Pela primeira vez, foram analisadas variações na composição molecular do secretoma antes e após a vitrificação de blastocistos humanos submetidos a PGT-A. Utilizando a análise de imunofluorescência (*Leprechaun*), identificaram-se exossomas específicos no secretoma embrionário, enriquecidos em tetraspaninas CD9, CD63 e/ou CD81, contendo fatores relacionados à pluripotência, implantação e apoptose.

Observou-se tendencialmente, no meio de cultura de embriões aneuploides um maior número de vesículas. Além disso, verificou-se que no meio de embriões euploides que resultaram em gravidez clínica apresentou mais vesículas HLA-G, fator associado à implantação, comparando com embriões não implantados. Resultados, estes, promissores na previsão da viabilidade e da probabilidade de implantação embrionária bem-sucedida, visando aprimorar as taxas de obtenção de gravidez clínica em TRA.

Plavras-chave: Teste Genético pré-implantacional (PGT); Blastocistos Humanos; Exossomas (Exo); Tetraspaninas; Biomarcadores.

Abstract

Effective embryo selection is crucial to enhance clinical pregnancy rates in assisted reproductive treatments (ART). Despite conventional selection criteria, based on morphokinetics or chromosomal status, the challenge of ensuring successful implantation persists, even with high-quality euploid embryos. Extracellular vesicles (EVs) production by in vitro-produced blastocysts has been correlated with the implantation process; however, no similar studies have been conducted on embryos following biopsy for preimplantation genetic testing for aneuploidy (PGT-A).

This study explores the embryonic secretome as a potential source of non-invasive biomarkers to identify suitable excellence embryos for transfer. First-ever, variations in the molecular composition of the secretome before and after vitrification of human blastocysts submitted to PGT-A were analysed. Using immunofluorescence analysis (*Leprechaun* machine), specific exosomes (Exo) in the embryonic secretome, enriched in CD9, CD63 and/or CD81 tetraspanins, were identified, containing factors related to pluripotency, implantation, and apoptosis.

A tendency was observed for aneuploid embryo spent culture media to contain more vesicles. Additionally, spent media from euploid embryos resulting in clinical pregnancy showed a higher number of HLA-G vesicles, an implantation-associated factor, compared to non-implanting embryos. These results hold promise for predicting the viability and likelihood of successful embryo implantation, aiming to improve clinical pregnancy rates in ART.

Keywords: Preimplantation Genetic Testing (PGT); Human Blastocysts; Exosomes (Exo); Tetraspanins; Biomarkers

Abbreviations and acronyms

ABs	Apoptotic bodies
AMA	Advanced Maternal Age
ART	Assisted Reproduction Treatments
ASEBIR	Association for the Study of Reproductive Biology
DNA	Deoxyribonucleic Acid
Epi	Epiblast
ESHRE	European Society of Human Reproduction and Embryology
EVs	Extracellular Vesicles
Exo	Exosomes
FET	frozen embryo transfer
GnRH	Gonadotropin-releasing hormone
GV	Germinal Vesicle
hCG	Human Chorionic Gonadotropin
HLA-G	Human Leukocyte Antigen G
ICSI	Intracytoplasmic Sperm Injection
ICM	Inner Cell Mass
ILVs	Intraluminal Vesicles
IVF	In Vitro Fertilisation
MI	Metaphase I
MII	Metaphase II
MVs	Microvesicles
MVEs	Multivesicular Endosomes
MHC	Histocompatibility Complex
NGS	Next-Generation Sequencing
PGD	Preimplantation Genetic Diagnosis
PGS	Preimplantation Genetic Screening
PGT	Preimplantation Genetic Testing
PGT-A	Preimplantation Genetic Testing for Aneuploidies
PGT-HLA	Preimplantation Genetic Testing for HLA histocompatibility complex
PGT-M	Preimplantation Genetic Testing for Monogenic diseases
PGT-SR	Preimplantation Genetic Testing for Structural Rearrangements
PFA	Paraformaldehyde
RIF	Recurrent Implantation Failure
RM	Recurrent Miscarriages
RNA	Ribonucleic Acid
SMF	Severe Male Factor
TE	Trophectoderm
TEMs	Tetraspanin-Enriched Microdomains
WHO	World Health Organization

General Index

Tables Index

Figures Index

Supplementary Tables Index

1. Introduction

According to the World Health Organization (WHO), infertility is a disorder of the male or female reproductive system characterized by the inability to conceive a pregnancy following 12 or more months of unprotected regular sexual intercourse. However, this period may be shortened to 6 months for women over 35 years of age. This adjustment is generally attributed to the notable decline in ovarian reserve, oocyte quality, and female fertility associated with advancing age. (Zegers-Hochschild et al., 2009)

Assisted Reproduction Treatments (ART) comprise a diverse range of specialized procedures developed to facilitate conception in cases of infertility, serving as an alternative for couples facing this condition.

1.1 Embryonic Development

An increasing adoption of elective single embryo transfer has been observed in reproductive medicine has been observed. This approach aims to select the embryo with the highest potential for successful implantation, increasing pregnancy success rates and mitigating complications associated with multiple gestation. (Hawke et al., 2021; Tomic et al., 2022) Throughout the years, the selection of the highest-quality embryo has been continuously improved. Morphokinetic assessment of the embryo entails a meticulous examination of morphological characteristics at regular intervals throughout its developmental progression. (Hawke et al., 2021) The embryos are graded based on the criteria of the Association for the Study of Reproductive Biology (ASEBIR), and can be classified as A, B, C, or D. (Hurtado de Mendoza et al., 2015) This selection process takes into account parameters including the number and symmetry of blastomeres (specific to the cellular stage), percentage of fragmentation, cell division rate, and degree of compaction. More specific features, such as the presence of cellular multinucleation are considered during this evaluation. (De Gheselle et al., 2022)

The morphokinetic study of embryos is the method of choice for many laboratories due to its cost-effectiveness, simplicity, rapidity, and non-invasiveness. However, there is no straightforward correlation between morphological features and the genetic composition of embryos.

The incidence of aneuploidies in human embryos is variable and can be influenced by various factors, including maternal age, with estimates suggesting it may occur in 20 to 80% of cases. (Tomic et al., 2022; Vera-Rodriguez et al., 2018) Thus, it is necessary to adopt an approach that accounts for this variability.

1.2 Preimplantation Genetic Testing (PGT)

In the 1960s, Edwards conceived the idea of Preimplantation Genetic Diagnosis (PGD). In collaboration with Gardner in 1967, they successfully stained the sexual chromatin present in rabbit blastocysts, subsequently visualizing it through fluorescence microscopy. (Edwards & Gardner, 1967) Due to the potential mutagenicity of this technique, which was incompatible with embryo transfer, in 1968, biopsies were conducted on 200 to 300 trophoblastic (TE) cells from rabbits, which were then subjected to staining for sexual chromatin. The biopsied blastocyst was subsequently implanted in a rabbit, and at the conclusion of the gestational period, the sex of the fetus was confirmed both anatomically and histologically. (Gardener & Edwards, 1968) This pioneering experiment laid the foundation for PGT and its application in the detection of genetically inherited diseases. (Vera-Rodriguez et al., 2018)

Only in 1990, were documented the first successful births following the implementation of PGD in human embryos. These initial cases of PGD involved couples at risk of transmitting hereditary genetic conditions linked to the X chromosome, such as adrenoleukodystrophy and X-linked mental retardation. Following in vitro fertilisation (IVF), a biopsy was conducted on a single cell from embryos at the 6 to 8-cell stage. Subsequently, PGD was performed, focusing on sex determination through DNA amplification of a specific repetitive sequence from the Y chromosome. This approach ensured the conception of female embryos, mitigating the risk of conceiving affected male embryos. In this context, XX embryos were transferred to the maternal uterus, culminating in the confirmation of a healthy twin pregnancy. (Handyside et al., 1990) Following this success in reproductive medicine, the application of the technique was expanded to encompass cases involving monogenic diseases or chromosomal anomalies. (Fuentes & Molina, 2007)

The European Society of Human Reproduction and Embryology (ESHRE) recently opted to simplify the terms Preimplantation Genetic Diagnosis (PGD) and Preimplantation Genetic Screening (PGS) by adopting the abbreviation PGT (Preimplantation Genetic Testing). (Kazuhiro Takeuchi, 2020) This technique provides couples with the opportunity to circumvent the challenging decision of terminating pregnancy in the face of embryos affected by severe genetic conditions. (Giuliano et al., 2023)

The initial phase of PGT encompasses embryonic biopsy, characterized by the retrieval of a small number of cell samples from an embryo for genetic analysis. Among the three main biopsy methodologies, trophectoderm (TE) biopsy in blastocyst-stage embryos, performed on the fifth or sixth day of development, is the most used. (Table 1) Embryonic biopsy is a two-step procedure, beginning with the perforation of the zona pellucida followed

by cell extraction for biopsy. (Table 1) Zona pellucida opening of the embryo (Assisted *Hatching*) can be achieved through various methods, with laser-assisted perforation being the most frequently adopted technique. The final extraction of the biopsy fragment may be conducted through various methods, including *Flicking* movement, *Pulling* technique, or *Laser* application. These methodologies aim to ensure an effective biopsy fragment while preserving the integrity of the embryo for subsequent procedures. (Table 1) (Giuliano et al., 2023)

Table 1 - Overview of techniques for embryonic biopsy procedures: Embryonic biopsy stages (Kokkali et al., 2020) *, Assisted embryonic hatching techniques (Aoyama & Kato, 2020) and Final embryonic biopsy fragment extraction techniques (Aoyama & Kato, 2020). Created with BioRender.com.*

Embryonic biopsy stages		
Polar body biopsy	Cleavage stage biopsy	Trophectoderm biopsy of a blastocyst-stage embryo
It involves the extraction and examination of the first and/or second polar bodies to assess the chromosomal status of an oocyte.	Usually performed on the third day post-fertilisation, it involves the extraction of one or two blastomeres (cells) from the embryo at the 6-8 cell stage.	It entails the extraction of a few cells, typically 5-10, from the trophectoderm of the blastocyst-stage embryo (day 5 or 6 of development).
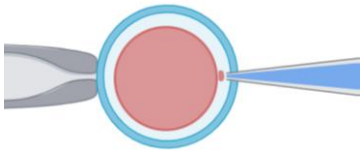	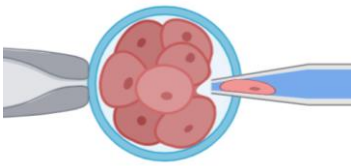	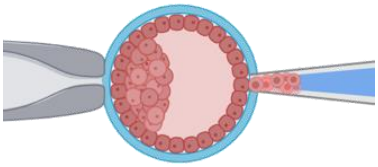
Assisted embryonic hatching techniques		
Mechanical Hatching	Chemical Hatching	Laser-assisted Hatching
It involves perforating the Zona Pellucida of the embryo using a micropipette.	It involves the utilization of an acidic solution to enzymatically dissolve the Zona Pellucida of the embryo.	It involves the use of a laser beam to generate a small opening in the Zona Pellucida of the embryo.
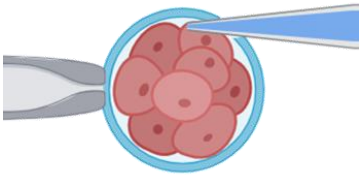	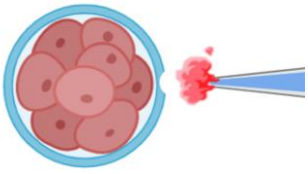	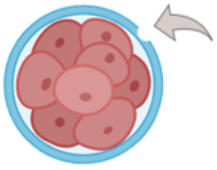

Final embryonic biopsy fragment extraction techniques		
Laser	*Flicking*	*Pulling*
It involves the utilization of a laser beam to remove the embryonic biopsy fragment.	It entails the extraction of the biopsy fragment through precise and swift movements of micropipettes.	It involves the removal of the biopsy fragment through a controlled stretching process.
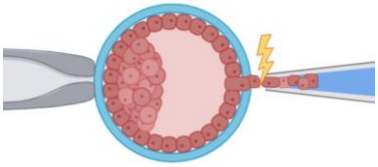	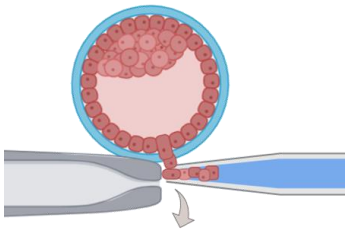	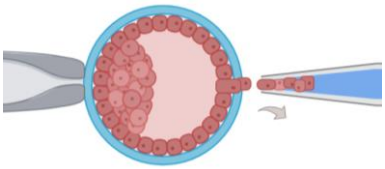

PGT can be subdivided into: PGT-M, for the detection of monogenic or mendelian hereditary diseases; PGT-SR, for the detection of structural chromosomal alterations, such as translocations and inversions; PGT-A, for the detection of numerical chromosomal abnormalities, such as aneuploidies; and recently, PGT-HLA, for the selection of embryos compatible with the HLA histocompatibility complex. (Kazuhiro Takeuchi, 2020)

1.2.1 Preimplantation genetic testing for chromosomal aneuploidies (PGT-A)

The frequent occurrence of aneuploidies, both in oocytes and embryos, significantly increases with maternal age advancement. The presence of these aneuploidies can lead to implantation failures or early spontaneous miscarriages. The selection of euploid embryos for transfer will contribute to improving implantation rates, diminish the occurrence of early miscarriages, and thereby elevate live birth rates, thus enhancing treatment efficacy. (Sordia-Hernandez et al., 2022; Tomic et al., 2022)

Preimplantation genetic testing for chromosomal aneuploidies (PGT-A) enables the identification of numerical abnormalities in chromosomes. It discerns the presence of additional copies of chromosomes, such as trisomy and polyploidies, while also capable of detecting the absence of copies of chromosomes, as observed in monosomies.

The main indications for performing this test include advanced maternal age (AMA), recurrent implantation failure (RIF) history, idiopathic recurrent miscarriages (RM), as well as the presence of severe male factor infertility (SMF). (Kokkali et al., 2020)

1.2.2 PGT-A results

There are 4 general types of results that PGT-A may include. The embryo can be classified as euploid, denoting the presence of the 23 pairs of chromosomes, which enables its selection for transfer owing to the increased probability of resulting in a successful

pregnancy and a healthy birth. (Figure 1) If the embryo exhibits an abnormal number of chromosomes, it is classified as aneuploid. (Figure 1) These embryos are generally not selected for transfer due to present genetic conditions incongruent with healthy development. (Taylor et al., 2014)

There is also a subtle probability of the embryo being classified as non-informative. This commonly arises from compromised genetic analysis, possibly due to the biopsy fragment being of insufficient dimensions for adequate analysis. (Figure 1) In this scenario, the responsible healthcare professional must conduct a thorough evaluation to determine if this embryo is eligible for transfer, considering the availability of healthy embryos for the couple. (Taylor et al., 2014)

Finally, when the embryo contains two or more genetically distinct cell lineages, it is considered mosaic. (Figure 1) Mosaicism commonly stems from post-zygotic mitotic errors during the embryonic developmental early stages. However, its manifestation in pre-implantation embryos does not necessarily denote the perpetuation of abnormal cell lineages throughout subsequent development. The transfer of such embryos is influenced by diverse factors, including the proportion of affected cells, constituting a subject of vigorous debate. (Taylor et al., 2014)

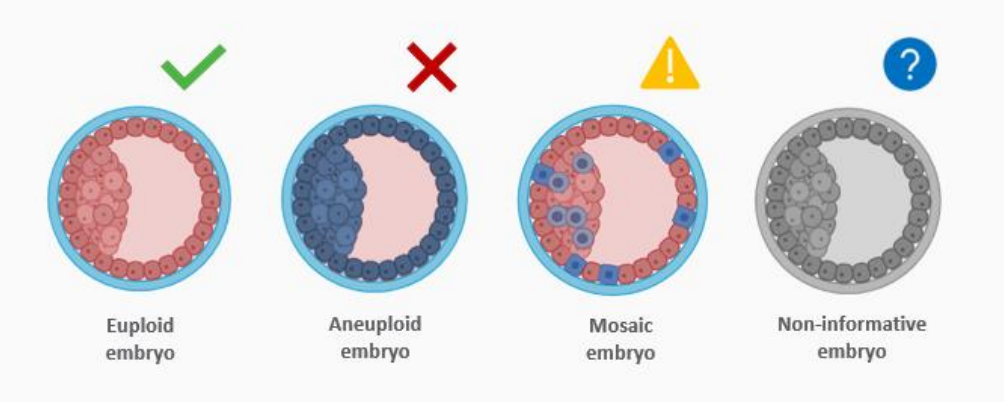

Figure 1 - Types of PGT-A outcomes during embryo analysis. From left to right: Euploid embryo (normal chromosome complement); Aneuploid embryo (abnormal chromosome complement); Mosaic embryo (mixed chromosome complement); Non-informative embryo (inconclusive result). Created with BioRender.com.

1.2.3 Genetic analysis

Presently, the prevailing technique for PGT-A involves invasive trophectoderm (TE) biopsy, followed by next-generation sequencing (NGS). (Giuliano et al., 2023) Genetic diagnosis via NGS represents an advanced methodology enabling comprehensive analysis of the embryo's entire genome, exhibiting high sensitivity in detecting genetic variations. (Parikh et al., 2018; Wells, 2014) The absence of standardization in genetic analysis

methods for PGT-A results in considerable variability in outcomes among different TRA clinics. (Tomic et al., 2022)

1.2.4 PGT-A limitations

As with any other methodology, PGT-A comes with certain limitations. It is a high-cost technique, demanding highly qualified professionals for its proper execution. To ensure the acquisition of a chromosomally normal embryo, certain patients may need to undergo multiple cycles of in vitro fertilization, incurring in substantial additional costs.

Although PGT-A is effective in detecting many chromosomal abnormalities, it is pertinent to note that it does not detect all genetic conditions, particularly those caused by point mutations. (Viotti, 2020) This test demonstrates a notable limitation in identifying mosaicism, characterized by the presence of multiple cell lineages in an embryo, which may result in the transfer of embryos with genetic anomalies. (Giuliano et al., 2023) Moreover, as with any diagnostic method, it presents the remote possibility of false positive or negative results, potentially leading to the inadvertent discarding of viable embryos or the transfer of an embryo with an undetected chromosomal anomaly. (Viotti, 2020)

Another significant limitation concerns the impact of the procedure on the embryo itself, as it involves the extraction of some of its cells, potentially causing damage to the embryo. Additionally, embryos biopsied on the fifth or sixth day of development must be cryopreserved, awaiting the availability of PGT-A results to program embryo transfer. (Cimadomo et al., 2016; Viotti, 2020)

This methodology also entails ethical and psychological aspects, as it involves the selection of embryos based on their genetic characteristics, which may emotionally impact the parents, especially in the face of abnormalities in their embryos. Even with this selection of apparently genetically normal embryos, there are no guarantees that this process will lead to a healthy pregnancy and birth, as additional factors beyond the genetic characteristics of the embryos can influence the implantation and consequently the pregnancy outcomes. (Giuliano et al., 2023)

1.3 Extracellular Vesicles (EVS)

Just like the majority of cell types, embryos secrete Extracellular Vesicles (EVs) delimited by a phospholipid bilayer. (Doyle & Wang, 2019; Zaborowski et al., 2015) These vesicles are recognized as an emerging medium of intercellular communication and are implicated in cellular homeostasis, coagulation, and waste removal. EVs possess the capacity to modulate both the physiological and pathological functions of recipient and

progenitor cells through intercellular transfer of proteins, lipids, and nucleic acids. (Colombo et al., 2014; Jankovičová, Sečová, et al., 2020; Van Niel et al., 2018)

EVs can be classified into three distinct main groups, based on criteria such as size, biogenesis, synthesis pathway, content, and function. These groups encompass apoptotic bodies (ABs), microvesicles (MVs), and exosomes (Exo). (Doyle & Wang, 2019; Kowalczyk et al., 2022)

1.3.1 Exosomes (Exo)

Exosomes represent the smallest subset of EVs, with a diameter ranging from 40-100 nm. The biogenesis of the endosomes typically initiates with invaginations of the cell membrane, a process known as endocytosis, forming endocytic vesicles. These vesicles subsequently merge to form early endosomes, which undergo maturation into multivesicular endosomes (MVEs). During this maturation process, additional invagination of the endosomal membrane occurs, resulting in the formation of intraluminal vesicles (ILVs) initially confined within the lumen of MVEs. The fusion of MVEs with the plasma membrane culminates in the release of ILVs into the extracellular microenvironment as Exo. (Figure 2) (El Andaloussi et al., 2013; Kowalczyk et al., 2022; Van Niel et al., 2018)

Exosomes contain a diverse array of biological constituents, including proteins, lipids and nucleic acids, reflecting their complexity and functional diversity. (Figure 2) (Kalluri & LeBleu, 2020)

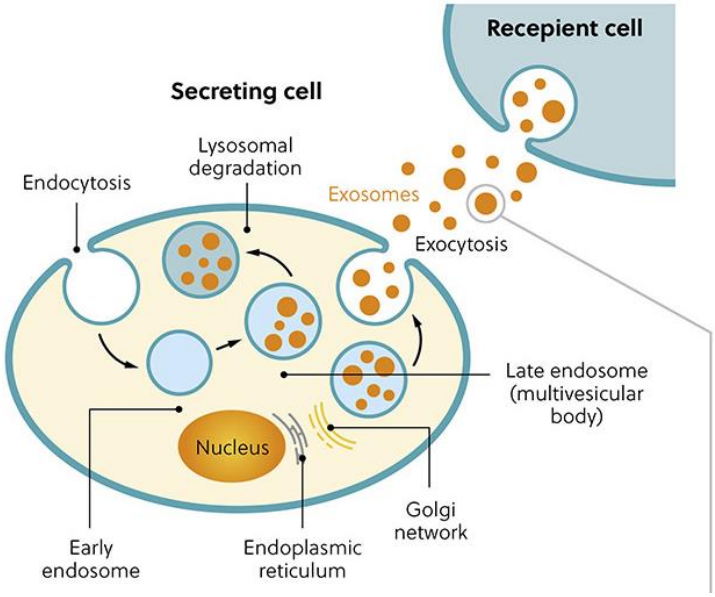

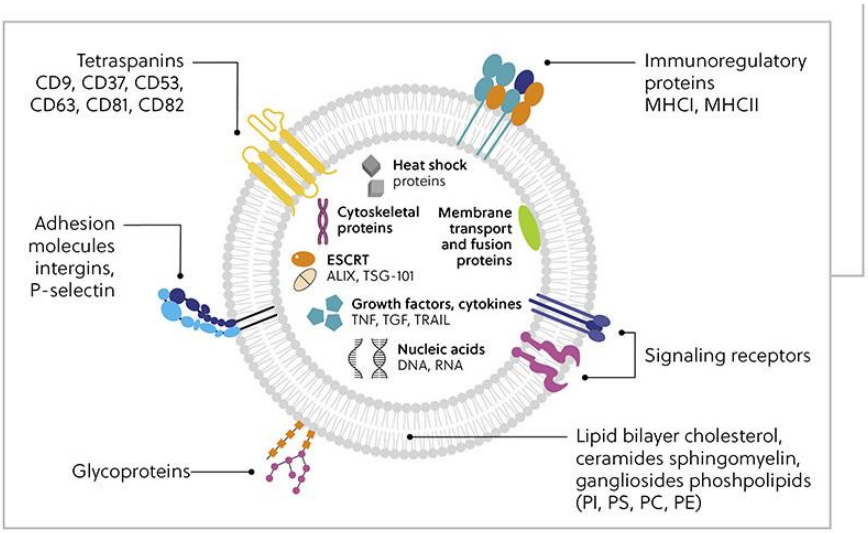

Figure 2 - Mechanism of Exosome Biogenesis and Molecular Composition (A) Schematic representation of the biogenesis and secretion of exosomes (Exo). (B) Schematic representation of the molecular components of Exo. Adapted from American Chemical Society (Tenchov, 2022).

The precise content of Exo may be influenced by the cellular origin type, cellular physiological state, environmental stimuli, and ongoing biological processes such as cellular signalling, cellular stress, immune response, and associated pathological conditions. Consequently, the analysis of Exo cargo assumes a significant role in comprehending their biological functions and their potential as biomarkers and therapeutic targets across diverse physiological and pathological contexts. (Jankovičová, Sečová, et al., 2020)

1.3.2 Tetraspanins

The tetraspanin family encompasses proteins integrated within the plasma membrane or within endosomal or lysosomal compartments of most cellular types. Characterized by a specific molecular structure, they are comprised of four transmembrane domains, two extracellular loops, one intracellular loop, and short cytoplasmic tails. (Figure 3) (Jankovičová, Sečová, et al., 2020; Toribio & Yáñez-Mó, 2022)

Through their extracellular, transmembrane, and cytoplasmic domains, tetraspanins establish interactions with other proteins, culminating in the formation of membrane protein clusters within tetraspanin-enriched microdomains (TEMs). (Jankovičová, Sečová, et al., 2020; Kummer et al., 2020) This organizational level is pivotal in numerous cellular processes, inclusive of Exo biogenesis. (Andreu & Yáñez-Mó, 2014; Kummer et al., 2020) Tetraspanins also engage in cellular signalling, adhesion, motility, fusion, activation, and cellular proliferation. (Termini & Gillette, 2017) Furthermore, their involvement has been observed in the pathogenesis of infections, the metastatic process in cancer, and their

fundamental contribution has been demonstrated in mammalian fertilization. (Charrin et al., 2014; Jankovičová, Neuerová, et al., 2020)

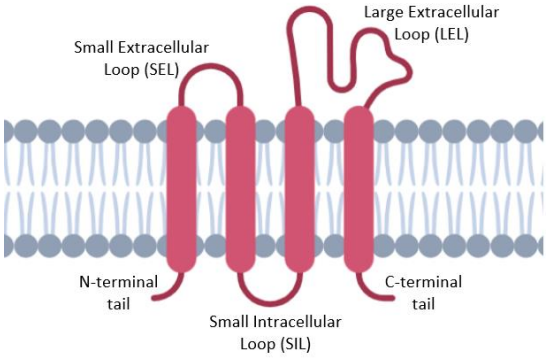

Figure 3 - Schematic representation of the molecular structure shared by of the tetraspanin family. These proteins are composed of a small extracellular loop (SEL), a large extracellular loop (LEL), a small intracellular loop (SIL), four transmembrane domains (TM1, TM2, TM3, and TM4), an intracellular loop, an N-terminal tail, and a C-terminal tail. Created with BioRender.com. (Balise et al., 2020; Karam et al., 2020)

Tetraspanins, including CD9, CD81, and CD63, are commonly used as specific markers for Exo populations owing to their heightened expression levels within these structures.(Jankovičová, Sečová, et al., 2020; Willms et al., 2018) Detection of these tetraspanins in the medium indicates the secretion of Exo by the embryonic cells, suggesting intercellular communication between the embryos and the surrounding environment. Furthermore, examination of the Exo within the medium can furnish pertinent data concerning the metabolic profile, cellular activity, and developmental potential of the embryos. (Jankovičová, Neuerová, et al., 2020)

Throughout human reproduction, tetraspanins are involved in several processes. They play a pivotal role in fertilization, coordinating sperm capacitation, acrosomal reaction, and sperm-egg fusion. Evidence suggests that their contribution to gamete maturation, encompassing both oogenesis and spermatogenesis. Tetraspanins persist in vital functions during early embryo development, participating in the genesis and arrangement of embryonic cells during initial cleavage and blastocyst formation. Moreover, they are also present during embryonic implantation in the uterine, mediating adhesion and intercellular communication between embryonic and endometrial cells, thereby facilitating successful implantation. Tetraspanins are thought to be important in syncytiotrophoblast formation, imperative for pregnancy establishment and maintenance.(Capra & Lange-Consiglio, 2020; Zhou et al., 2022) Notably, research into the release of Exo containing these tetraspanins in the uterine environment has garnered greater attention compared to exosomal release by gametes or embryos, highlighting a significant lacuna in comprehension of this domain.

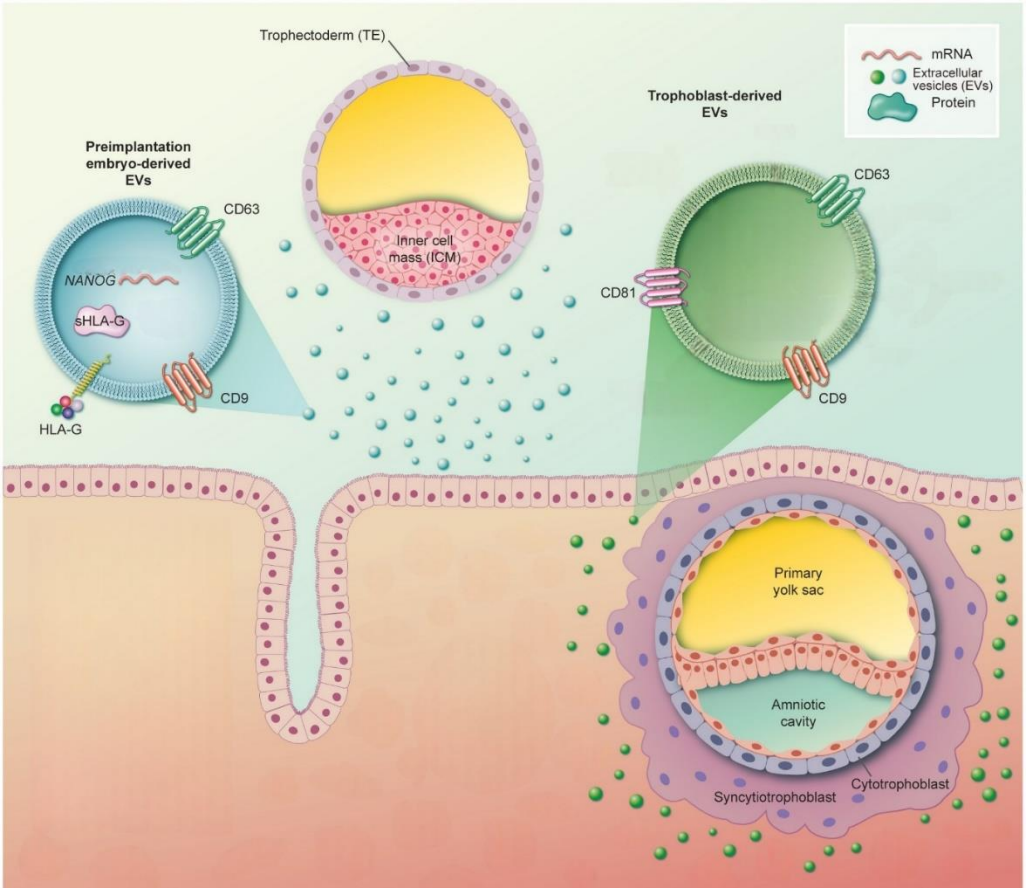

Figure 4 - Schematic representation of extracellular vesicles (EVs) derived from preimplantation embryos and trophoblasts. Adapted from (Giacomini et al., 2019).

1.3.2.1 CD9

The appropriate presence of tetraspanin CD9 is crucial for the normal embryonic development and the formation of the tissues composing the fetus and placenta. (Liu et al., 2006) Modifications in its expression can affect embryonic viability and pregnancy progression. The presence of CD9 has been showed on the surface of mice blastocyst TE cells, along with its identification within extracellular vesicles (EVs) located on the plasma membrane, perivitelline space, and zona pellucida, as well as its release into the extracellular environment. (Figure 4) (Giacomini et al., 2017; Jankovičová, Sečová, et al., 2020; Vyas et al., 2019) This protein is implicated in maternal-fetal communication, being involved in the migration and cellular invasion of the blastocyst during the implantation process in the uterine endometrium. (Giacomini et al., 2017; Vyas et al., 2019) It participates in the regulation of signalling pathways that promote cellular mobility and interaction with the uterine environment, playing a crucial role in regulating the production of enzymes like MMP 2, engaged in cellular invasion during embryonic implantation.(Liu et al., 2006)

1.3.2.2 CD63

The detection of CD63 in the blastocoel fluid of human blastocysts and in EVs suggests that this tetraspanin serves as a cellular signalling molecule and mediates communication between the embryo and the uterine endometrium during the implantation process. (Figure 4) (Battaglia et al., 2019; Jankovičová, Neuerová, et al., 2020) CD63 contributes to the establishment of cellular junctions and interactions with adhesion molecules within the uterine environment. Additionally, it serves as a regulator of cellular signalling, modulating intracellular and intercellular signalling pathways that impact the response of blastocyst cells to environmental and intrauterine stimuli by interacting with cell surface receptors and signalling proteins. (Ng et al., 2013)

1.3.2.3 CD81

The dysregulation of CD81 signalling contributes to abnormal blastocyst placentation. This tetraspanin has been detected in EVs within the blastocoel fluid of human blastocysts, indicating its involvement in cellular communication.(Battaglia et al., 2019) Specifically, CD81 has been shown to play a crucial role in membrane fusion during syncytiotrophoblast formation, a specialized tissue at the embryo-endometrium interface during implantation, facilitating blastocyst adhesion and invasion. (Shen et al., 2017)

1.3.3 Nanog

During embryonic development, the appropriate expression of the homeobox gene (transcription factor) Nanog is crucial for maintaining cellular pluripotency, additionally playing a pivotal role in regulating cell differentiation throughout fetal development. (Figure 4) (Allègre et al., 2022; Lee et al., 2023; Shahbazi et al., 2020; Zhang et al., 2016) Nanog exhibits high expression levels in the inner cell mass (ICM) of the human blastocyst, playing an essential role in initiating differentiation of the epiblast (Epi) cells. (Allègre et al., 2022; Giacomini et al., 2017; Karam et al., 2020; Lee et al., 2023) This facilitates the coordinated expression of pluripotency factors such as SOX2, OCT4, and KLF4 through a mechanism that remains incompletely understood. (Allègre et al., 2022; Lee et al., 2023) The NANOG expression profile in humans closely resembles that observed in mice. (Hambiliki et al., 2012) Evidence from mice embryos lacking Nanog suggests that ICM cells in the blastocyst fail to differentiate into viable epiblasts (Epi), resulting in the unviability of these embryos. These findings underscore the importance of Nanog in maintaining pluripotency during preimplantation embryo development, rendering it a valuable marker for assessing embryonic viability. (Mitsui et al., 2003; Shahbazi et al., 2020; Silva et al., 2009)

1.3.4 Human Leukocyte Antigen G (HLA-G)

The human leukocyte antigen G (HLA-G) is a member of the major histocompatibility complex (MHC) and is accountable for immunological tolerance and modulation of the immune response. (Niu et al., 2017)

The bidirectional communication between the maternal uterus and the blastocyst during embryo implantation and subsequent pregnancy is paramount for the progression of the processes of apposition, adhesion, fixation, and penetration of the embryo. Evidence over the years suggests that factors of embryonic origin may facilitate the adherence of the blastocyst to the endometrium and its invasion into the uterine lining. (Giacomini et al., 2017)

Two pivotal factors for a successful pregnancy are maternal-fetal immune tolerance and early embryo development and implantation. Part of the MHC antigens present in fetal cells are inherited from the father. Consequently, the maternal immune system may recognize these antigens as foreign and trigger an immune response against the fetus, leading to pregnancy complications such as miscarriage. To mitigate this immune response, both fetal and placental cells of maternal origin naturally produce proteins such as HLA-G, which participate in maternal-fetal immune tolerance during pregnancy, protecting the fetus from recognition and attack by the maternal immune system.(Kotze et al., 2013; Roussev & Coulam, 2007)

In the human blastocyst, TE cells express HLA-G, which plays a fundamental role in the initial attachment and embryonic implantation in the maternal uterus. (Figure 4) (Giacomini et al., 2017) Moreover, the presence of HLA-G associated with extracellular vesicles (EVs) derived from pre-implantation human embryos has been demonstrated. (Giacomini et al., 2019) During TE cell invasion, HLA-G regulates cytokine secretion, thereby promoting a local immunosuppressive state. (Giacomini et al., 2019; Roussev & Coulam, 2007) Evidence has been documented indicating that HLA-G contributes to embryonic immune tolerance, embryo development, adhesion, and invasion during embryonic implantation, as well as upregulating HCG expression in TE. (Wang et al., 2013) Therefore, the presence of HLA-G in the culture medium of human embryos may be regarded as a candidate molecular biomarker for evaluating the implantation potential and the probability of clinical pregnancy of these embryos. (Niu et al., 2017)

1.3.5 Annexin-V

Apoptosis, also referred to as programmed cell death, is a natural process occurs during normal embryonic development to maintain the delicate balance between cell proliferation and cell demise, imperative for successful development. However, excessive, or aberrant occurrences of apoptosis can compromise embryo viability. This process eliminates

damaged, unnecessary, or potentially harmful cells and can be triggered by diverse factors, including genetic damage, oxidative stress, suboptimal culture conditions, or abnormal embryonic development. (Ramos-Ibeas et al., 2020)

Embryonic quality is usually associated with reduced apoptotic rates. Cellular fragmentation observed in embryos represents a morphological alteration linked to the induction of cellular apoptosis, potentially diminishing embryo viability when present in heightened levels. (Levy et al., 1998; Ramos-Ibeas et al., 2020) Additionally, embryos with chromosomal abnormalities tend to demonstrate an increased predisposition to apoptosis. (Ramos-Ibeas et al., 2020)

Annexin-V is a protein that binds to phosphatidylserine, a phospholipid exposed on the outer surface of the lipid bilayer of the cell membrane during the initial stages of the apoptotic pathway, rendering it a specific biochemical marker for discerning cellular apoptosis. (Ramos-Ibeas et al., 2020; Vermes et al., 1995) (Figure 5) In a study conducted in 2017 by Pallinger et al., EVs positive for Annexin V were detected in spent culture media from human embryos, suggesting a potential association between the presence of Annexin V and embryonic competence. Monitoring Annexin V levels in culture media could provide valuable insights into the developmental status and health of embryos, aiding in the selection of competent embryos for transfer. (Pallinger et al., 2017)

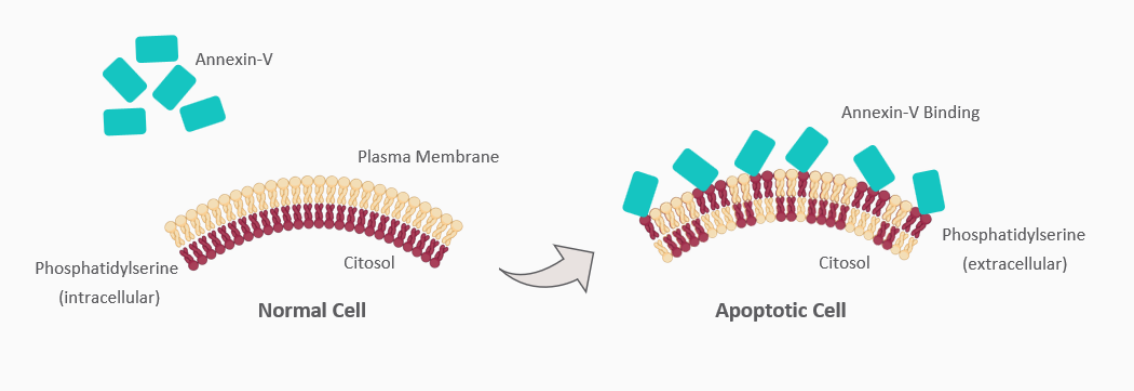

Figure 5 - Schematic representation of the apoptotic process showing the induction of apoptosis, translocation of phosphatidylserines to the outer leaflet of the cytoplasmic membrane, and the binding of annexin V to exposed phosphatidylserine residues. This process leads to the flipping of phospholipids and serves as a key mechanism for the recognition and clearance of apoptotic cells by phagocytes. Created with BioRender.com.

This study explores the embryonic secretome as a potential source of non-invasive biomarkers to identify suitable excellence embryos for transfer. For the first time, variations in the molecular composition of the secretome before and after vitrification of human blastocysts submitted to PGT-A were analysed. Using immunofluorescence analysis

(Leprechaun machine), specific exosomes (Exo) in the embryonic secretome, enriched in CD9, CD63 and/or CD81 tetraspanins, were identified, containing factors related to pluripotency (Nanog), implantation (HLA-G), and apoptosis (Anexinn-V).

The specific objectives of this dissertation are as follows: Evaluate the production of extracellular vesicles by blastocysts subjected to trophectoderm biopsy for PGT-A; Characterize the proteomic composition in tetraspanins of secreted vesicles; Molecularly characterize the embryonic secretome pre- and post-vitrification process; Correlate the production of vesicles by blastocysts with the incubation time in the culture medium; Compare extracellular vesicle production between euploid and aneuploid embryos; and Correlate the production of factors related to pluripotency, implantation, and apoptosis with clinical pregnancy rates.

2. Methodologies

2.1 Experimental design

This study encompasses two cohorts of samples: those obtained post preimplantation genetic testing executed on embryos, prior to their vitrification – Group 1 (n=48 samples, derived from embryo culture media of 17 distinct couples); and those obtained post-thawing of the euploid embryo designated for uterine transfer – Group 2 (n=32 samples, obtained from embryo culture media of 31 distinct couples). Eight couples are common to both sample cohorts. (Schema 1)

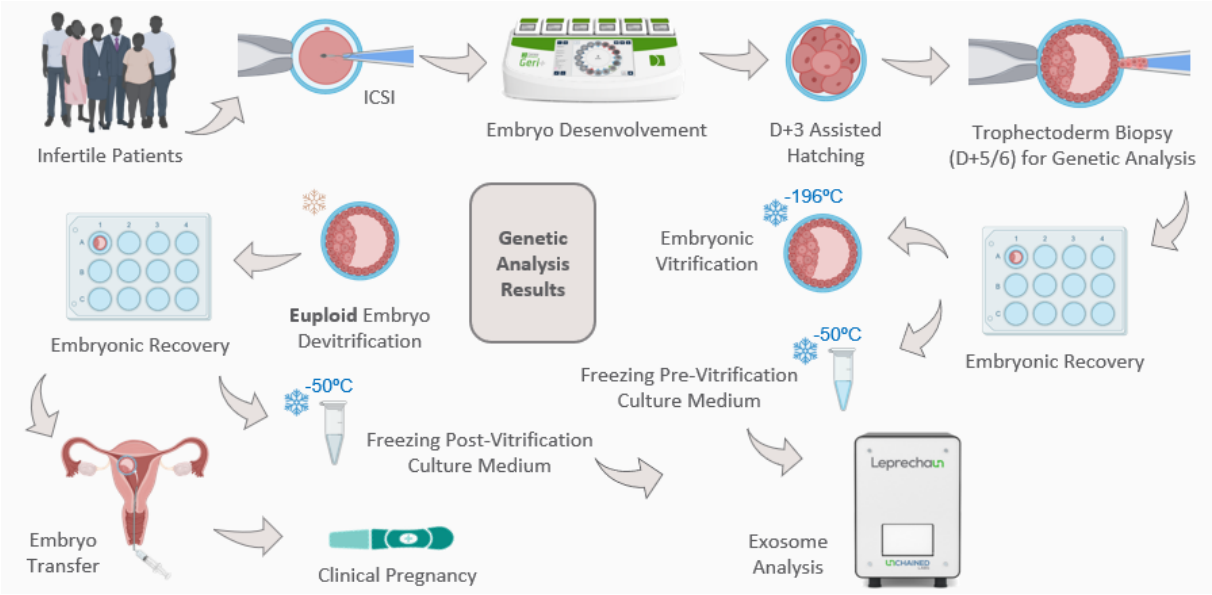

Schema 1 - Experimental Design Resume. Created with BioRender.com.

2.2 Patients Selection

The current study involved the selection of participants from couples seeking fertility treatment at the Extremadura Institute of Assisted Reproduction (IERA) - QuironSatud in Badajoz, Spain. The research was conducted between December 2023 and June 2024, using culture media from embryos designated for preimplantation genetic testing (PGT) as part of assisted reproduction treatment. The patients couples included in this study ranged in age from 28 to 51 years and had experienced unsuccessful clinical pregnancy following unprotected sexual intercourse for a minimum of 12 consecutive months.

Informed consent for the procedures and collection of clinical data was obtained from all participating patients. The study received approval from the local ethics committee of the Extremaduran Institute of Assisted Reproduction (IERA) - QuironSalud in Badajoz. The

characteristics of the embryos and the clinical data of the respective patients involved in the study are detailed in the supplementary table 1 to 4.

2.3 Gamete Retrieval and Embryo Selection for Biopsy

In this study, patients underwent controlled ovarian stimulation using either a gonadotropin-releasing hormone (GnRH) agonist or antagonist protocol. Ovarian follicles were retrieved transvaginally under ultrasonographic guidance, 36 hours after human chorionic gonadotropin (hCG) administration for ovulation induction. Follicle denudation was achieved using enzymatic and mechanical methods, followed by assessment of oocyte maturation stage (MII, MI, GV). Semen processing involved concentration gradients or the ZYMOT method, particularly in cases of significant sperm fragmentation. Mature oocytes (MII) underwent intracytoplasmic sperm injection (ICSI) with a single carefully selected spermatozoon, based on morphology and motility criteria. Subsequently, newly injected oocytes were transferred to a culture dish in a time-lapse incubator (Geri®) for monitoring of fertilization and embryonic development in the subsequent days. On the third day post-fertilization, assisted hatching of selected embryos for PGT was performed using laser. (Schema 1)

Embryonic quality was evaluated according to morphokinetic criteria established by ASEBIR. On the fifth or sixth day of development, only blastocysts exhibiting a high degree of embryonic expansion, along with ICM and TE graded as A, B, or C, were considered eligible for TE biopsy for preimplantation genetic testing (PGT).

2.4 Preimplantation Genetic Testing (PGT) and Exosome Isolation

The embryonic biopsy procedure entailed the extraction of five to ten cells from the TE of the blastocyst on the fifth or sixth day of development, employing laser technology. The embryonic laser application did not surpass three pulses, and the biopsy fragment was extracted utilizing the *Flicking* or *Pulling* method to ensure adequate process completion. After the biopsy procedure, the embryo underwent a single wash and was transferred to a post-biopsy culture dish containing SAGE 1-Step^{TM} medium (Cooper Surgical). This dish was maintained in an incubator at 37°C and 6.0% CO_2, providing the optimal conditions for complete embryo recovery. (Schema 1)

The biopsy fragment underwent a tubing process, which entailed the intubation of the collected cells. The tubes containing the samples were stored at -50ºC and sent to the IGENOMICS or BIORRAY laboratory, specialized in genetic analysis of biopsied cells using next-generation sequencing (NGS). The results of this analysis were obtained after an approximate period of 15 days.

The embryo's resting period was recorded, and subsequently, the embryo was vitrified following the Kitazato Cryotop® protocol. The embryo resting medium (20uL) was pipetted into appropriately labelled Eppendorf tubes, along with 180ul of DPBS 1x (Gibco™). These tubes were stored at -50ºC until analysis.

2.5 Embryo Transfer and Exosome Isolation

At this Assisted Reproduction Centre, single euploid embryo transfer is the preferred approach. During the embryo transfer procedure, the highest quality euploid embryo is thawed according to Kitazato Cryotop® protocol. Following thawing, the embryo is maintained in SAGE 1-Step™ culture medium (Cooper Surgical) for approximately 2 hours. Following this period of recovery, the embryo is transferred into the maternal uterus using a catheter under ultrasound guidance. Post-transfer, the embryo's resting medium (20µL) is pipetted into appropriately labelled Eppendorf tubes, along with 180µL of DPBS 1x (Gibco™), and stored at -50ºC. (Schema 1)

2.6 Pregnancy Assessment

Approximately 10 days after embryo transfer, the patient undergoes a urine pregnancy test and serum hCG levels are measured to confirm pregnancy. A negative result in both tests indicates a lack of clinical pregnancy. In the case of a positive urine test but serum hCG levels fail to confirm pregnancy, it is considered a biochemical pregnancy loss. Conversely, concurrent positive results in both tests confirm clinical pregnancy. Around 20 days post-transfer, these patients undergo ultrasonography to verify pregnancy, which is evidenced by the presence of one or more gestational sacs and fetal heartbeat detection.

2.7 Exosome Analysis for Tetraspanins (CD9, CD63, CD81)

For exosome analysis, the LEPRECHAUN machine from Unchained Labs was used. Samples were equilibrated to room temperature for 15 minutes. Subsequently, 25µL of sample along with 25µL of incubation solution, were dispensed onto the chip (luni) for incubation at room temperature for approximately 16 hours.

After the incubation period of the samples on the chips, 1mL of solution A was added, followed by 3 washes of 3 minutes each with the same solution (removing 750uL of the sample solution and replacing it with 750uL of solution A in each wash). Subsequently,

The tetraspanin antibody cocktail with 5µL antibody of CD9, CD63 and CD81 diluted at 1:240 in blocking solution, was supplemented to the chips for 1 hour of agitation. A last wash of the chips was performed using solution A, followed by three washes with solution B and a final wash with distilled water for 3 minutes, using a shaker. Individually, the chips

were gently immersed in distilled water and placed to dry on filter paper. At last, the chips were analysed using the LEPRECHAUN machine from Unchained Labs.

2.8 Exosome Analysis for Nanog, HLA-G and Annexin-V

For exosome analysis, the LEPRECHAUN machine from Unchained Labs was used. Samples were equilibrated to room temperature for 15 minutes. Subsequently, 25µL of sample along with 25 µL of incubation solution, were dispensed onto the chip (luni) for incubation at room temperature for approximately 16 hours.

After the incubation period of the samples on the chips, 1mL of solution A was added, followed by 3 washes of 3 minutes each with the same solution (removing 750uL of the sample solution and replacing it with 750uL of solution A in each wash). Subsequently, 250uL of Annexin-V Antibody (diluted at 1:480 with blocking solution) was added to the chips, covered with aluminium foil, and agitated for 15 minutes. Three additional washes with solution A were performed, followed by the addition of 4% Paraformaldehyde (PFA) to the chips for fixation for 10 minutes under agitation. After three additional washes with solution A, permeabilization was carried out with 0.5% Saponin for 10 minutes under agitation. Three more washes with the same solution were executed, and then the Nanog and HLA-g antibody cocktail (diluted at 1:300 and 1:120 in blocking solution, respectively) was supplemented to the chips for 1 hour of agitation. Finally, a last wash of the chips was performed using solution A, followed by three washes with solution B and a final wash with distilled water for 3 minutes, using a shaker. Individually, the chips were gently immersed in distilled water and placed to dry on filter paper. At last, the chips were analysed using the LEPRECHAUN machine from Unchained Labs.

2.9 Exosome Analysis with the Laprechaun Machine Unchained Labs

Leprechaun captures exosomes using their surface proteins, such as cd9, cd63 and cd81 tetraspanins, and assessing their size by interferometry technique (IM). Furthermore, by employing capture antibodies tagged with immunofluorescence, can detect the pater of tetraspanins in the exosomes or factors within the exosomes, including Nanog, Hla-g and Annexin-v.

In each chip, there are three designated spots for capturing each tetraspanin (cd9, cd63 and cd81), along with an additional spot for in-specific capture acting as a negative control of the samples (MlgG1). Additionally, each spot is labelled with fluorescence for the detection of the pater of tetraspanins in the exosomes (Figure 5) or the detection of factors such Nanog, HLA-G and Annexin-v. (Figure 6) The exosome concentration obtained for each tetraspanin is calculated as the average of three, ensuring a more precise evaluation.

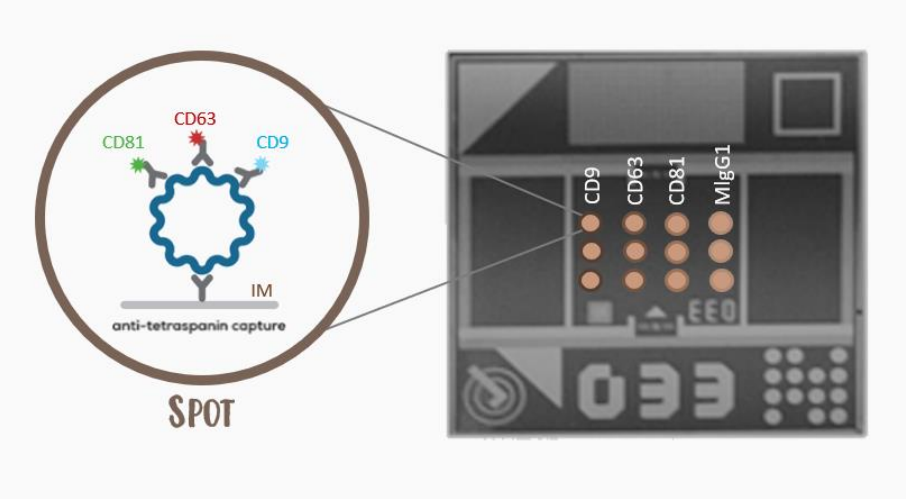

Figure 6 - Leprechaun analysis of exosomes in the chip, with tetraspanina antibodies. Created with BioRender.com.

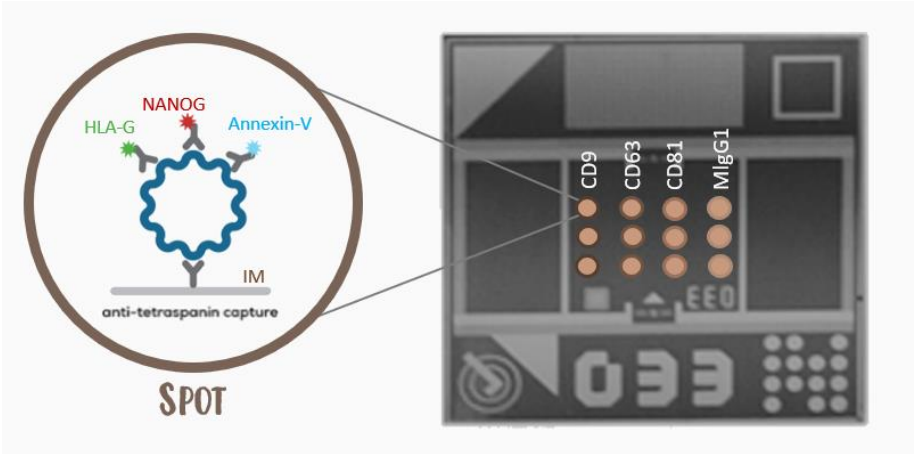

Figure 7 - Leprechaun analysis of exosomes in the chip, with Nanog, Hla-G and Annexin-V antibodies. Created with BioRender.com.

2.10 Statistical Analysis

To enhance result precision and mitigate error, every chip encompasses three analysis sites per sample. This methodology allows for a more accurate mean estimation of vesicle quantities in each sample, given that each undergoes tripartite analysis.

The student's t-test and analysis of variance (ANOVA) were employed as appropriate. Contingency tables were executed using Fisher's exact test. A statistical significance threshold of $P < 0.05$ was adopted. All analyses were conducted employing IBM SPSS Statistics 29.0.2.0 software (IBM Corp., Armonk, NY, USA).

3. Results

3.1 Patients Characteristics

3.1.1 Post-Biopsy Group – Group 1

In this cohort, spent culture media from 48 blastocysts, which were biopsied for Preimplantation Genetic Testing (PGT) prior to vitrification, were collected. These embryos were derived from 17 infertile couples. The number of blastocysts per treatment cycle varied from 1 to 9, with the most common outcome being 1 blastocyst per cycle (n=7).

The indications for PGT screening included advanced maternal age (47.1%), Severe male factor infertility (35.3%), recurrent miscarriage (17.6%), and recurrent implantation failure (11.8%), with multiple diagnoses possible per couple. Maternal ages ranged from 28 to 48 years, while paternal ages ranged from 33 to 51 years. (Table 2)

3.1.2 Post-Desvitrification Group – Group 2

In this group, the spent culture media from 32 euploid blastocysts post-devitrification for embryo transfer in frozen cycles have been collected to date. These blastocysts originated from 31 infertile couples. Maternal age at the time of transfer ranged from 28 to 48 years. (Table 2)

The characteristics of embryonic development, including morphokinetics, ploidy status, and the clinical features of the patients and treatment cycles are detailed in supplementary table 1 to 4.

Table 2 - Clinical outcomes in patients who underwent PGT-A cycles. body mass index (BMI); advanced maternal age (AMA); severe male factor (SMF); recurrent miscarriages (RM); recurrent implantation failure (RIF); estradiol (E2); follicle stimulating hormone (FSH).

Characteristic	Description Group 1	Description Group 2
Couple Patients, n	17	31
Maternal age (years)	39 ± 3,7	37,6 ± 4,3
Maternal BMI (Kg/m2)	21,1 ± 3,0	22,3 ± 2,7
Duration of infertility (years)	1,7 ± 1,0	2,3 ± 1,2
Type of infertility, n (%)		
Primary	12 (70,6%)	27 (84,4%)
Secondary	4 (23,5%)	5 (15,6%)
Number of prior pregnancies (n)	5	15
Nº of prior embryos transfers (n)	5	14
Seminogram, n (%)		

Normozoospermia	10	19
Normozoospermia (Donor)	-	3
Asthenozoospermia	-	1
Teratozoospermia	1	3
OligoAsthenozoospermia	1	-
OligoTeratozoospermia	1	-
AsthenoTeratozoospermia	1	-
OligoAsthenoTeratozoospermia	3	6
Indication for PGT-A, n (%)		
AMA	8 (47,1%)	11 (34,4%)
MSF	6 (35,3%)	9 (28,1%)
RM	3 (17,6%)	8 (25,0%)
RIF	2 (11,8%)	4 (12,5%)
Transfer Characteristics, mean ± Sd		
E2 levels (IU/L)	-	225,8 ± 220,8
FSH levels (IU/L)	-	21,1 ± 8,0
Endometrial thickness on transfer day (mm)	-	10,1 ± 1,9

3.2 Embryo Characteristics

Table 3 - Embryological outcomes of embryos undergoing biopsy for PGT-A: A comparative analysis of Group 1 (pre-vitrification embryos) and Group 2 (post-devitrification embryos).

Characteristic	**Description Group 1**	**Description Group 2**
Embryo Spent Medium Recovered, n	48	32
Time in Spent Medium Culture (min)	30,3 ± 14,9	137,8 ± 16,4
Blastocysts PGT-A results, n (%)		
Euploid	22 (45,8%)	32 (100%)
Aneuploid	25 (52,1%)	-
Mosaic	1 (2,1%)	-
Embryonic development day for biopsy, n (%)		
Day 5	40 (83,3%)	25 (78,1%)
Day 6	8 (16,7%)	7 (21,9%)
Embryo Quality, n (%)		
Blastocyst AA	3 (6,3%)	6 (18,8%)
Blastocyst AB	8 (16,7%)	7 (21,9%)
Blastocyst BA	2 (4,2%)	1 (3,1%)
Blastocyst BB	24 (50,0%)	10 (31,3%)
Blastocyst BC	6 (12,5%)	3 (9,4%)
Blastocyst CB	4 (8,3%)	5 (15,6%)
Blastocyst CC	1 (2,1%)	0 (0,0%)
Desenvolvement Failures		
Multinucleation	21 (43,8%)	-
Fragmentation	17 (35,4%)	-
Number of euploid Transfers, n (%)		
Implantation rate	-	20 (69,0%)

3.2.1 Post-Biopsy Group – Group 1

The duration that embryos remained in the spent culture medium following biopsy ranged from 6 to 80 minutes, with a mean duration of 30 minutes. (Table 3)

The embryonic developmental stage was recorded, with 40 (83.3%) embryos reaching the blastocyst stage on day five, and an additional 8 (16.7%) embryos attaining the blastocyst stage on day six. Fifty percent of the blastocysts were assigned a morphokinetic grade of BB for both the inner cell mass (ICM) and the trophectoderm (TE).

The chromosomal status of the tested embryos indicated that 45.8% were diagnosed as euploid (n = 22). Only 2.1% of the blastocysts analysed (n = 1) were classified as mosaic, whereas 52.1% were identified as aneuploid (n = 25). Among the aneuploid group, 11 embryos exhibited monosomy, 11 exhibited trisomy, and 3 presented a combination of monosomy and trisomy. (Table 3)

The correlations between embryo euploidy rates, blastocyst development day, morphokinetic quality, and developmental anomalies such as multinucleation are presented in Table 4.

Among the 40 embryos that attained the blastocyst stage on day 5 of development, 21 (52.5%) were euploid. In contrast, of the 8 blastocysts analysed on day 6, only 1 (12.5%) was euploid. Although the difference did not achieve statistical significance (p = 0.052), there is a noticeable trend indicating that embryos reaching the blastocyst stage on day 5 exhibit a higher proportion of euploidy compared to those reaching this stage on day 6.

In this analysis, embryos were stratified into three morphokinetic quality categories: A (highest quality), B (good quality), and C (low quality). The comparison of euploidy rates among these categories unveiled that embryos of quality A demonstrated a superior euploidy rate (63.6%) in contrast to those of quality B (43.8%) and quality C (20%).

The percentage of euploid embryos exhibiting cellular fragmentation during their development (47.0%) was comparable to that of euploid embryos devoid of such fragmentation (46.7%).

Of the 48 embryos subjected to embryonic biopsy, 21 displayed multinucleation, of which 8 (38.1%) were classified as euploid. Subsequent analysis of the 13 multinucleated aneuploid embryos revealed that 8 (61.5%) were classified with monosomy, 3 (23.1%) with trisomy, and 2 (15.4%) exhibited both conditions concurrently. Furthermore, embryos with multinucleation with three or more nuclei within a single cell (n = 8) exhibited a significant association with higher rates of aneuploidy (p = 0.008). These 8 embryos originated from women aged over 37 years.

Table 4 - Embryological Outcomes: A comparative analysis of Euploid and Aneuploid blastocysts from Group 1 (pre-vitrification embryos).

Characteristic		Euploid	Aneuploid	TOTAL
PGT Results		22 (45,8%)	25	47
Embryonic development day for biopsy, n (%)				
Day 5		21 (52,5%)	18	39
Day 6		1 (12,5%)	7	8
Embryo Quality, n (%)				
Blastocyst AA	A	7 (63,6%)	3	11
Blastocyst AB				
Blastocyst BA	B	14 (43,8%)	18	32
Blastocyst BB				
Blastocyst BC				
Blastocyst CB	C	1 (20,0%)	4	5
Blastocyst CC				
Disinvolvement Failures				
Without Fragmentation		14 (46,7%)	16	30
With Fragmentation		8 (47,0%)	9	17
Without Multinucleation		14 (53,8%)	12	26
With Multinucleation		8 (38,1%)	13	21
2 Nuclei		8 (61,5%)	5	13
3 Nuclei		0 (0%)	5	5
3 and 4 Nuclei		0 (0%)	2	2
4 Nuclei		0 (0%)	1	1

3.2.2 Post-Transfer Group – Group 2

Thus far, the spent culture media from 25 euploid blastocysts at day five of development (78.1%) and 7 euploid blastocysts at day six of development (21.9%) have been collected following devitrification. The predominant embryonic quality among these blastocysts was classified as BB for both the inner cell mass (ICM) and the trophectoderm, observed in 31.3% of cases. The clinical pregnancy rate was 69.0% (n=20) per euploid embryo transferred. Following devitrification, embryos remained in the culture medium for a duration ranging from 120 to 180 minutes, with an average of 138 minutes. (Table 3)

The associations among the clinical implantation rate, blastocyst developmental stage on the day of embryo transfer, and morphokinetic embryo quality are described in Table 5.

Among the 23 euploid blastocysts implanted on the fifth day of development, 17 (73.9%) achieved clinical pregnancy. In contrast, of the 6 blastocysts implanted on day 6, only 3 (50.0%) achieved clinical pregnancy.

The blastocysts transferred with morphokinetic grade A exhibited a clinical pregnancy rate of 58.3%, while those classified as grade B demonstrated a higher rate of

84.6%. Conversely, blastocysts classified as grade C resulted in clinical pregnancy in 50.0%. of cases.

Table 5 - Embryological Outcomes: A comparative analysis of Implantation and no Implantation blastocyst from Group 2 (post-devitrification embryos).

Characteristic		Implantation	No Implantation	TOTAL
Implantation rate		20 (69,0%)	9	29
Embryonic development day for biopsy, n (%)				
Day 5		17 (73,9%)	6	23
Day 6		3 (50,0%)	3	6
Embryo Quality, n (%)				
Blastocyst AA	A	7 (58,3%)	5	12
Blastocyst AB				
Blastocyst BA	B	11 (84,6%)	2	13
Blastocyst BB				
Blastocyst BC				
Blastocyst CB	C	2 (50,0%)	2	4
Blastocyst CC				

3.3 Tetraspanin Analysis

The dimensions and quantities of exosomes isolated from 23 samples of spent culture medium from blastocysts, which undergoing biopsy for PGT before vitrification (Group 1) and after devitrification (Group 2), were analysed. Exosomes expressing the tetraspanins CD9, CD63, and CD81 on their surfaces were captured and subsequently labelled with fluorescent antibodies targeting the same tetraspanins, to quantify their presence in the medium.

In the two cohorts, a uniformity was observed in the proportions of vesicles captured across the four capture channels, with a predominance of vesicles displaying the tetraspanin CD63 on their surfaces. Comparable quantities were captured in the CD81 and MIgG1 channels. (Table 6)

In both groups, vesicles captured in the CD63 and CD81 channels predominantly exhibit only that specific tetraspanin on their surface. The proportion of CD63 only vesicles in the CD63 channel was 44.9% for group 1 and 38.1% for group 2. For CD81 only vesicles in the CD81 channel, this proportion was 52.7% for group 1 and 52.0% for group 2. In the capture channel for exosomes expressing tetraspanin CD9 on their surface, a higher capture rate of vesicles containing both CD9 and CD81 (50.6% and 51.1% in group 1 and 2, respectively) was observed compared to vesicles containing only the tetraspanin CD9 (33.6% and 29.2% in group 1 and 2, respectively). (Table 6)

A slightly higher prevalence of captured vesicles was noted in the samples from group 2 compared to those from group 1. (Table 6)

Regarding interferometry (IM), the percentage of analysed vesicles relative to the total number of vesicles captured in each channel was approximately 19% for group 1 and 8% for group 2. (Table 6)

Table 6 - Exossome Analysis: A comparative Tetraspanin analysis in the spent medium of Group 1 (pre-vitrification embryos) and Group 2 (post-devitrification embryos).

Tetraspanin Analysis	Description Group 1	Description Group 2
Embryos Analysed, n	23	23
Sample dilution	1:20	1:20
Capture Exosomes in CD9 Chanel, mean ± Sd (%)	179,7 ± 88,7	248,3 ± 103,3
CD9	59,6 ± 43,3 (33,6%)	72,5 ± 48,9 (29,2%)
CD9 and CD63	26,6 ± 12,9 (15,0%)	43,8 ± 10,0 (17,6%)
CD9 and CD81	89,9 ± 75,3 (50,6%)	127,0 ± 53,2 (51,1%)
CD9, CD63 and CD81	1,4 ± 1,4 (0,8%)	5,0 ± 7,3 (2,0%)
IM	(20,7%)	(9,3%)
Size (nm)	55,1 ± 7,0	57,0 ± 10,0
Capture Exosomes in CD63 Chanel, mean ± Sd (%)	404,0 ± 179,8	557,7 ± 178,1
CD63	181,5 ± 94,8 (44,9%)	212,7 ± 60,7 (38,1%)
CD9 and CD63	80,5 ± 75,8 (19,9%)	133,1 ± 108,5 (23,9%)
CD63 and CD81	140,9 ± 98,7 (34,9%)	206,3 ± 89,7 (37,0%)
CD9, CD63 and CD81	1,1 ± 0,7 (0,3%)	5,7 ± 6,9 (1,0%)
IM	(14,6%)	(6,9%)
Size (nm)	54,5 ± 7,8	60,0 ± 11,8
Capture Exosomes in CD81 Chanel, mean ± Sd (%)	114,3 ± 43,6	192,7 ± 71,7
CD81	60,3 ± 33,1 (52,7%)	100,3 ± 43,5 (52,0%)
CD9 and CD81	32,4 ± 18,7 (28,3%)	49,9 ± 28,6 (25,9%)
CD63 and CD81	20,1 ± 10,3 (17,6%)	34,3 ± 9,9 (17,8%)
CD9, CD63 and CD81	1,6 ± 2,3 (1,4%)	8,4 ± 17,2 (4,3%)
IM	(21,8%)	(8,8%)
Size (nm)	60,1 ± 14,2	59,8 ± 10,9
Capture Exosomes in MIgG1 Chanel, mean ± Sd	125,2 ± 46,2	174,4 ± 78,0

The detailed results of the tetraspanin exosome analysis are presented in supplementary table 5 and 6.

3.4 Analysis of Nanog, HLA-G and Annexin-V

Thus far, 12 samples of spent culture medium from blastocysts undergoing biopsy for PGT prior to vitrification (Group 1) and 8 samples post-devitrification (Group 2) have been analysed. Exosomes expressing the tetraspanins CD9, CD63, and CD81 on their surfaces were captured and subsequently labelled with fluorescent antibodies to detect the presence of Nanog, HLA-G, and Annexin-V.

There were no discernible disparities in vesicle quantity between the same channels in Group 1 and Group 2. (Table 7)

Table 7 - Exossome Analysis: A comparative Nanog, HLA-G and Annexin-V analysis in the spent medium of Group 1 (pre-vitrification embryos) and Group 2 (post-devitrification embryos).

Analysis	Description Group 1	Description Group 2
Embryos Analysed, n	12	8
Sample dilution	1:20	1:20
Capture Exosomes in CD9 Chanel, mean ± Sd	482,0 ± 159,2	501,9 ± 106,8
Nanog	272,3 ± 56,9	217,5 ± 39,6
HLA-G	138,4 ± 149,3	196,3 ± 121,8
Annexin-V	60,7 ± 11,2	71,6 ± 18,1
Nanog and HLA-G	1,6 ± 1,8	2,9 ± 2,5
Nanog and Annexin-V	6,0 ± 2,1	5,8 ± 4,1
HLA-G and Annexin-V	1,8 ± 1,9	3,6 ± 5,5
Nanog, HLA-G and Annexin-V	1,3 ± 1,2	4,4 ± 8,4
Capture Exosomes in CD63 Chanel, mean ± Sd	662,5 ± 105,7	569,9 ± 118,3
Nanog	374,5 ± 69,8	265,8 ± 60,0
HLA-G	167,8 ± 45,0	206,8 ± 128,6
Annexin-V	101,0 ± 24,8	77,3 ± 20,2
Nanog and HLA-G	2,4 ± 2,7	3,5 ± 1,6
Nanog and Annexin-V	7,8 ± 3,2	5,8 ± 2,6
HLA-G and Annexin-V	4,5 ± 11,2	2,1 ± 1,6
Nanog, HLA-G and Annexin-V	4,3 ± 9,4	2,5 ± 1,9
Capture Exosomes in CD81 Chanel, mean ± Sd	453,3 ± 63,1	444,4 ± 119,6
Nanog	296,7 ± 50,8	229,25 ± 62,1
HLA-G	84,9 ± 30,5	161,87 ± 148,7
Annexin-V	62,7 ± 11,7	46,4 ± 6,4
Nanog and HLA-G	0,5 ± 0,5	2,0 ± 1,9
Nanog and Annexin-V	5,9 ± 1,5	3,5 ± 2,6
HLA-G and Annexin-V	1,6 ±1,8	0,5 ± 0,5
Nanog, HLA-G and Annexin-V	0,8 ± 1,2	0,7 ± 0,7
Capture Exosomes in MIgG1 Chanel, mean ± Sd	407,5 ± 168,3	385,0 ± 65,5

The detailed results of the exosome analysis for Nanog, HLA-G and Annexin-V are presented in supplementary table 7 and 8.

3.4.1 Post-Biopsy Group – Group 1

In this cohort, a slightly higher incidence of captured vesicles was detected in the samples derived from aneuploid embryos compared to those from Euploid embryos. The

presence of Nanog is comparable in both euploid and aneuploid samples, regardless of the capture channel. (Table 8)

Table 8 - Exossome Analysis: A comparative Nanog, HLA-G and Annexin-V analysis of Euploid and Aneuploid spent medium blastocysts from Group 1 (pre-vitrification embryos).

Analysis	Euploid	Aneuploid
Embryos Analysed, n	4	8
Capture Exosomes in CD9 Channel, mean ± Sd	449,25 ± 69,4	498,4 ± 192,0
Nanog	298,5 ± 61,6	259,3 ± 53,5
HLA-G	85,5 ± 7,0	164,9 ± 180,6
Annexin-V	56,0 ± 13,9	63,0 ± 9,8
Capture Exosomes in CD63 Channel, mean ± Sd	627,0 ± 62,3	680,3 ± 121,6
Nanog	373,5 ± 12,3	375,0 ± 87,1
HLA-G	137 ± 15,9	183,1 ± 47,5
Annexin-V	83,8 ± 26,5	109,6 ± 20,3
Capture Exosomes in CD81 Channel, mean ± Sd	428,0 ± 59,7	466,0 ± 64,7
Nanog	294,0 ± 39,8	298,0 ± 58,0
HLA-G	70,0 ± 8,0	92,4 ± 35,2
Annexin-V	57,5 ± 15,3	65,3 ± 9,5

3.4.2 Post-Transfer Group – Group 2

In general, a slight trend was observed for embryos that failed to implant exhibit a greater abundance of detected vesicles in the spent medium. (Table 9)

Specifically, there appeared to be a tendency for a higher concentration of vesicles expressing HLA-G on their surface in embryos that led to implantation and, consequently, clinical pregnancy.

Table 9 - Exossome Analysis: A comparative Nanog, HLA-G and Annexin-V analysis of Implantation and no Implantation spent medium blastocysts from Group 2 (post-devitrification embryos).

Analysis	Implantation	No Implantation
Embryos Analysed, n	5	3
Capture Exosomes in CD9 Chanel, mean ± Sd	485,6 ± 124,3	529,0 ± 85,2
Nanog	205,0 ± 40,1	238,3 ± 34,9
HLA-G	206,6 ± 144,2	179,0 ± 98,4
Annexin-V	64,8 ± 13,2	83,0 ± 22,1
Capture Exosomes in CD63 Chanel, mean ± Sd	556,8 ± 138,5	591,7 ± 97,4
Nanog	247,6 ± 69,6	296,0 ± 26,2
HLA-G	220,2 ± 150,7	184,3 ± 105,9

Annexin-V	67,6 ± 17,8	93,3 ± 12,9
Capture Exosomes in CD81 Chanel, mean ± Sd	480,6 ± 137,2	384,0 ± 60,6
Nanog	224,8 ± 56,0	236,7 ± 84,0
HLA-G	200,8 ± 178,6	97,0 ± 59,0
Annexin-V	47,2 ± 1,6	45,0 ± 11,5

4 Discussion

4.1 Embryo Characteristics

The formation of blastocysts on the fifth day of embryonic development frequently correlates with elevated rates of euploidy, showing superior genetic quality. Conversely, blastocysts achieving this stage on the sixth day of development tend to manifest a heightened prevalence of aneuploidy. (Florensa et al., 2024; Li et al., 2022) This tend suggests that the timing of blastocyst formation could serve as a potential marker of embryo genetic quality. (Yee & Tian, 2019) The present study, although constrained by sample size, revealed findings consistent with existing literature. Among the embryos analysed, those developing to the blastocyst stage on day 5 (52.5%) manifested a superior euploidy rate relative to blastocysts reaching formation on day 6 (12.5%). (Table 3) These results suggest that embryonic developmental speed may be a crucial feature to consider in embryo selection for transfer, potentially enhancing clinical success rates in *in vitro* fertilisation practices.

The assessment of embryonic quality is a routine practice in in vitro fertilisation (IVF) laboratories, entailing the classification of blastocysts into distinct morphokinetic categories based on the evaluation of Inner Cell Mass (ICM) and Trophectoderm (TE). Recent research indicates that embryos with superior morphological characteristics are more likely to be euploid, suggesting that morphology may serve as a reflection of the chromosomal integrity of embryos. (Florensa et al., 2024; Li et al., 2022) Discrepancies in euploidy rates among distinct embryological quality groups underscore the importance of morphology as a potential indicator of embryonic genetic competence. Although the present study necessitates a larger sample size for robust statistical validation, the preliminary results are consistent with previously reported findings in the literature. Embryos with superior morphokinetic quality demonstrated higher euploidy rates compared to those of lower quality, underscoring the importance of morphological criteria in the selection of embryos for transfer.

Embryonic multinucleation is characterised by the presence of multiple nuclei within at least one blastomere during early developmental stages, particularly at the two- or four-cell stage. Previous studies suggest that multinucleation may be indicative of genetic instability, potentially compromising the embryo's developmental competence and its ability to achieve successful implantation and a viable pregnancy. (Arrones-Olmo et al., 2017; Bamford et al., 2022; Ergin et al., 2014; Papadopoulou et al., 2021) This morphological feature has been associated toa diminished competence in embryo developmental, potentially stemming from irregular distribution of genetic material during initial cell divisions.

Nonetheless, the correlation between multinucleation and euploidy remains a subject of intense debate and scientific investigation. While certain studies propose an association between multinucleation and aneuploidy, this relationship lacks complete understanding and demands further investigation for clarification. (Papadopoulou et al., 2021)

In aneuploid embryos exhibiting multinucleation, monosomies were more commonly observed than trisomies, suggesting a specific pattern of chromosomal instability. (Balakier et al., 2016) The outcomes of this investigation validate such trend, with 61.5% of multinucleated embryos displaying monosomies and 23.1% manifesting trisomies.

The occurrence of two nuclei within a dividing cell is not entirely unexpected, as it can be attributed to an ongoing cell division process where the nuclei have not yet completely separated. Additionally, studies have demonstrated that binucleated embryos exhibit higher rates of high-quality blastocyst formation, as well as increased pregnancy and live birth rates. (Talbot et al., 2022) However, the presence of three or more nuclei within a single cell may be a more robust indicator of genetic instability or chromosomal anomalies. In this study, multinucleated embryos were classified based on the number of nuclei present, revealing significant differences in aneuploidy rates between the groups. Embryos exhibiting multinucleation with three or more nuclei within a single cell demonstrated a significant association with higher aneuploidy rates ($p = 0.008$). Specifically, out of 48 embryos biopsied, 8 displayed multinucleation with three or more nuclei, all of which were identified as aneuploid. (Table 4) This observation suggests a correlation between the extent of multinucleation and the presence of chromosomal abnormalities. The existing literature of embryonic multinucleation is limited, particularly regarding distinctions based on the number of nuclei. These results emphasise the necessity for further research to elucidate the clinical implications of multinucleation in human embryos. The correlation observed suggest that multinucleation, particularly in cases involving three or more nuclei, could potentially serve as a biomarker for the exclusion of aneuploid embryos, providing a rapid and non-invasive selection method for ART.

Euploid blastocysts, irrespective of their developmental stage, demonstrate comparable probabilities of implantation. This implies that, given their euploidy status, it is advantageous to consider their transfer regardless of the developmental day. (Yee & Tian, 2019) Nevertheless, this study observed a clinical pregnancy rate of 73.9% for euploid embryos transferred on day 5 of development, in contrast to a clinical pregnancy rate of 50.0% for embryos transferred on day 6. (Table 5) Recent research demonstrates that when selecting an embryo for transfer in a frozen embryo transfer (FET) cycle, embryos cryopreserved on day 5 are more likely to result in live births compared to those cryopreserved on day 6. These findings suggest that the rate of development at which an

embryo reaches a mature blastocyst stage is a superior predictor of outcome in FET cycles than morphological classification. (Bourdon et al., 2019; Malmsten et al., 2018)

According to the data collected in this study, no significant differences were identified between the three embryo morphological classification groups in relation to implantation rates. (Table 5) However, recent studies have shown that, in relation to morphological factors, there is a significant correlation between the degree of inner cell mass (ICM) and the embryo implantation rate. (Benlioglu et al., 2023)

4.2 Tetraspanin Analysis

Tetraspanins, including CD9, CD81, and CD63, are commonly used as specific markers for Exo populations owing to their heightened expression levels within these structures. (Jankovičová, Sečová, et al., 2020; Willms et al., 2018) In this study, a higher prevalence of vesicles exhibiting the tetraspanin CD63 on their surfaces was noted in comparison to those expressing CD9 and CD81. This tetraspanin molecule functions as a cellular signalling molecule mediator, orchestrating communication between the embryo and the uterine endometrium throughout the implantation process and it is present in extracellular vesicles (EVs) and the blastocoel fluid.(Battaglia et al., 2019; Jankovičová, Neuerová, et al., 2020) A possible explanation for the abundance of this tetraspanin may lie in the hypothesis that, subsequent to embryonic biopsy, the blastocell fluid may disperse into the surrounding environment, resulting in an increased concentration of this tetraspanin in the medium.

Furthermore, the surface manifestation of tetraspanin CD9 on vesicles has been documented in the spent medium of human embryos subjected to embryonic biopsy, both pre- and post-vitrification stages. (Table 6) Noteworthy observations have been documented regarding the presence of these tetraspanins on the trophoectoderm (TE) cell surface of mice blastocysts, indicating their pivotal role in maternal-fetal communication during uterine implantation processes. (Giacomini et al., 2017; Jankovičová, Sečová, et al., 2020; Vyas et al., 2019)

In both Group 1 and Group 2, the concentration of vesicles captured via the CD81 channel (114.3 vs. 192.7) mirrors that of nonspecifically captured vesicles by the negative control capture channel MIgG1 (125.2 vs. 174.4, respectively). (Table 6) This suggests a modest presence of this tetraspanin in the spent medium of embryos undergoing embryonic biopsy for preimplantation genetic testing (PGT) before and after vitrification. A possible explanation for this lies in the essential role played by this tetraspanin in the formation of the syncytiotrophoblast during embryo implantation. (Shen et al., 2017) In this context, considering the early developmental stage of the biopsied embryos, it is expected that they

will not yet show significant expression of this tetraspanin on the surface of their exosomes. This observation emphasises the relevance of the temporal context and the stage of embryonic development in assessing the expression of specific proteins, such as tetraspanins, in the spent media of embryos, highlighting the complexity of embryonic development.

As demonstrated in Table 6, in both groups, vesicles captured in the CD63 and CD81 channels predominantly exhibit only the specific tetraspanin on their surface. This indicates that these tetraspanins are reliable markers for detecting other markers present in the vesicles. In the capture channel for exosomes expressing tetraspanin CD9 on their surface, a higher capture rate of vesicles containing both CD9 and CD81 was observed compared to vesicles containing only the tetraspanin CD9. This suggests that tetraspanin CD9 may not be an adequate specific marker for detecting other markers present in the vesicles, as the results may be more correlated with the presence of tetraspanin CD81 in this specific case.

A slightly higher prevalence of captured vesicles was noted in the samples from Group 2 compared to those from Group 1. This difference can be attributed to the substantially longer recovery period in the culture medium for the embryos in Group 2 (mean of 138 minutes) compared to those in Group 1 (mean of 30 minutes), thereby providing a prolonged interval for vesicle secretion in Group 2. However, despite this observation, the disparity in vesicle concentration between the groups is not significant. (Table 6)

Given the association of tetraspanins (CD9, CD63, CD81) with the embryonic implantation process, it is plausible to assume an increase in their expression in embryos that resulted in pregnancy (Liu et al., 2006). However, it was not possible to establish a correlation between the number of vesicles expressing these tetraspanins and the rates of euploidy or implantation in Groups 1 and 2, respectively.

The technique of interferometry (IM) enables the precise measurement of the size of vesicles captured by tetraspanins in the capture channels, ranging between 35 and 200 nm in diameter. However, in this study, a discrepancy was observed between the number of vesicles analysed by interferometry (IM) and those retained in the capture channels. This suggests that most of the vesicles in the samples fall outside this size range, most likely having dimensions smaller than 35 nm. This conclusion is supported by the fact that the mode of the vesicles analysed in IM is around 40 nm, approaching the lower detectable limit of this technique. (Table 6)

Nonetheless, a study published by Cambridge University Press was able to measure the average diameter of MVs/Exo present in spent media from human embryos

using nanoparticle tracking analysis. It was found that the diameter of vesicles from quality A embryos was larger compared to quality B and C embryos, with the mean vesicle diameter being approximately 105 nm (Veraguas et al., 2020). This diameter does not align with the results obtained in this study.

4.3 Analysis of Nanog, HLA-G and Annexin-V

Between Groups 1 and 2, the concentration of vesicles present in the spent culture medium showed no significant variation following the vitrification process. (Table 7)

While this study requires a larger sample size for robust statistical validation, a subtle trend is discernible indicating that aneuploid embryos tend to exhibit a higher vesicle count, regardless of the expression of Nanog, HLA-G, or Annexin-V. (Table 8) Studies indicate that the incidence of apoptosis is elevated in the media of aneuploid embryos and mosaic embryos compared to that of euploid embryos. (Martín et al., 2024)

Furthermore, there is evidence indicating that embryos secrete higher levels of sHLA-G before vitrification compared to after devitrification. (Radwan et al., 2022) To validate these hypotheses, a larger sample size would be necessary for analysis.

A subtle trend was observed where embryos failing to implant tended to exhibit a greater abundance of detected vesicles in the spent medium. Conversely, embryos resulting in pregnancy and/or live birth following transfer showed increased secretion of sHLA-G compared to those where transfer concluded without pregnancy. (Radwan et al., 2022) This study exhibits a slight inclination in this direction. (Table 9)

5 Conclusion

In summary, this study scrutinised molecular composition variations of the secretome before and after vitrification of human blastocysts undergoing PGT-A. It pinpointed specific extracellular vesicles within the embryonic secretome, enriched in tetraspanins CD9, CD63, and/or CD81, harbouring factors associated with pluripotency, implantation, and apoptosis.

Despite its limited sample size, this study yields findings consistent with existing literature. It serves as an initial exploration into analysing spent culture medium from embryos subjected to embryonic biopsy for PGT. Given the brief project duration, it remains in the developmental phase, with potential for additional data inclusion to yield more robust conclusions. As a roadmap for future research, investigating these markers (Tetraspanins, Nanog, HLA-G, Annexin-V) via alternative methodologies such as Enzyme-Linked Immunosorbent Assay (ELISA), exploring additional biomarker types present in embryonic

vesicles, such as microRNAs, or expanding the sample size to encompass a more diverse population, would be beneficial. Such endeavours could pave the way for utilising the embryonic secretome as a non-invasive biomarker source for discerning top-tier embryos suitable for transfer, ultimately augmenting clinical pregnancy rates in ART.

6 References

Allègre, N., Chauveau, S., Dennis, C., Renaud, Y., Meistermann, D., Estrella, L. V., Pouchin, P., Cohen-Tannoudji, M., David, L., & Chazaud, C. (2022). NANOG initiates epiblast fate through the coordination of pluripotency genes expression. *Nature Communications*, *13*(1). https://doi.org/10.1038/s41467-022-30858-8

Andreu, Z., & Yáñez-Mó, M. (2014). Tetraspanins in extracellular vesicle formation and function. *Frontiers in Immunology*, *5*(SEP). https://doi.org/10.3389/fimmu.2014.00442

Aoyama, N., & Kato, K. (2020). Trophectoderm biopsy for preimplantation genetic test and technical tips: A review. In *Reproductive Medicine and Biology* (Vol. 19, Issue 3, pp. 222–231). John Wiley and Sons Ltd. https://doi.org/10.1002/rmb2.12318

Arrones-Olmo, S., Genoves, A., Martinez, I., & Cuevas, I. (2017). Importance of multinucleation at the two-cell stage in embryo development. *Fertility and Sterility*, *108*(3), e151–e152. https://doi.org/10.1016/j.fertnstert.2017.07.459

Balakier, H., Sojecki, A., Motamedi, G., & Librach, C. (2016). Impact of multinucleated blastomeres on embryo developmental competence, morphokinetics, and aneuploidy. *Fertility and Sterility*, *106*(3), 608-614.e2. https://doi.org/10.1016/j.fertnstert.2016.04.041

Balise, V. D., Saito-Reis, C. A., & Gillette, J. M. (2020). Tetraspanin Scaffold Proteins Function as Key Regulators of Hematopoietic Stem Cells. In *Frontiers in Cell and Developmental Biology* (Vol. 8). Frontiers Media S.A. https://doi.org/10.3389/fcell.2020.00598

Bamford, T., Barrie, A., Montgomery, S., Dhillon-Smith, R., Campbell, A., Easter, C., & Coomarasamy, A. (2022). Morphological and morphokinetic associations with aneuploidy: a systematic review and meta-analysis. In *Human Reproduction Update* (Vol. 28, Issue 5, pp. 656–686). Oxford University Press. https://doi.org/10.1093/humupd/dmac022

Battaglia, R., Palini, S., Vento, M. E., La Ferlita, A., Lo Faro, M. J., Caroppo, E., Borzì, P., Falzone, L., Barbagallo, D., Ragusa, M., Scalia, M., D'Amato, G., Scollo, P., Musumeci, P., Purrello, M., Gravotta, E., & Di Pietro, C. (2019). Identification of extracellular vesicles and characterization of miRNA expression profiles in human blastocoel fluid. *Scientific Reports*, *9*(1). https://doi.org/10.1038/s41598-018-36452-7

Benlioglu, C., Keles, I., Kalafat, E., Ata, B., & Bozdag, G. (2023). Time-lapse morphokinetic parameters and implantation outcomes of single euploid embryo transfers. *Reproductive BioMedicine Online*, *47*, 103473. https://doi.org/10.1016/j.rbmo.2023.103473

Bourdon, M., Pocate-Cheriet, K., Finet De Bantel, A., Grzegorczyk-Martin, V., Amar Hoffet, A., Arbo, E., Poulain, M., & Santulli, P. (2019). Day 5 versus Day 6 blastocyst transfers: A systematic review and meta-analysis of clinical outcomes. *Human Reproduction*, *34*(10), 1948–1964. https://doi.org/10.1093/humrep/dez163

Capra, E., & Lange-Consiglio, A. (2020). The biological function of extracellular vesicles during fertilization, early embryo—maternal crosstalk and their involvement in reproduction: Review and overview. In *Biomolecules* (Vol. 10, Issue 11, pp. 1–26). MDPI AG. https://doi.org/10.3390/biom10111510

Charrin, S., Jouannet, S., Boucheix, C., & Rubinstein, E. (2014). Tetraspanins at a glance. *Journal of Cell Science*, *127*(17), 3641–3648. https://doi.org/10.1242/jcs.154906

Cimadomo, D., Capalbo, A., Ubaldi, F. M., Scarica, C., Palagiano, A., Canipari, R., & Rienzi, L. (2016). The Impact of Biopsy on Human Embryo Developmental Potential during

Preimplantation Genetic Diagnosis. In *BioMed Research International* (Vol. 2016). Hindawi Limited. https://doi.org/10.1155/2016/7193075

Colombo, M., Raposo, G., & Théry, C. (2014). Biogenesis, secretion, and intercellular interactions of exosomes and other extracellular vesicles. In *Annual review of cell and developmental biology* (Vol. 30, pp. 255–289). https://doi.org/10.1146/annurev-cellbio-101512-122326

De Gheselle, S., Jacques, C., Chambost, J., Blank, C., Declerck, K., De Croo, I., Hickman, C., & Tilleman, K. (2022). Machine learning for prediction of euploidy in human embryos: in search of the best-performing model and predictive features. *Fertility and Sterility*, *117*(4), 738–746. https://doi.org/10.1016/j.fertnstert.2021.11.029

Doyle, L. M., & Wang, M. Z. (2019). Overview of extracellular vesicles, their origin, composition, purpose, and methods for exosome isolation and analysis. In *Cells* (Vol. 8, Issue 7). MDPI. https://doi.org/10.3390/cells8070727

Edwards, R. G., & Gardner, R. L. (1967). Sexing of live rabbit blastocysts. *Nature*, *214*, 576–577.

El Andaloussi, S., Mäger, I., Breakefield, X. O., & Wood, M. J. A. (2013). Extracellular vesicles: Biology and emerging therapeutic opportunities. In *Nature Reviews Drug Discovery* (Vol. 12, Issue 5, pp. 347–357). https://doi.org/10.1038/nrd3978

Ergin, E. G., Çalişkan, E., Yalçinkaya, E., Öztel, Z., Çökelez, K., Özay, A., & Özörnek, H. M. (2014). Frequency of embryo multinucleation detected by time-lapse system and its impact on pregnancy outcome. *Fertility and Sterility*, *102*(4), 1029-1033.e1. https://doi.org/10.1016/j.fertnstert.2014.06.030

Florensa, M., Cladellas, A., Ballesteros, A., & Esbert, M. (2024). Preimplantation genetic testing for aneuploidy: predictive embryonic factors. *Journal of Assisted Reproduction and Genetics*. https://doi.org/10.1007/s10815-024-03061-5

Fuentes, F. J. R., & Molina, M. P. R. (2007). Diagnóstico genético preimplantacional. *Revista Española de PEDIATRÍA Clínica e Investigación*, *63*(6), 443–449.

Gardener, R. L., & Edwards, R. G. (1968). Control of the sex ratio at full term in the rabbit by transferring sexed blastocysts. *Nature*, *218*, 346–348.

Giacomini, E., Alleva, E., Fornelli, G., Quartucci, A., Privitera, L., Vanni, V. S., & Viganò, P. (2019). Embryonic extracellular vesicles as informers to the immune cells at the maternal–fetal interface. In *Clinical and Experimental Immunology* (Vol. 198, Issue 1, pp. 15–23). Blackwell Publishing Ltd. https://doi.org/10.1111/cei.13304

Giacomini, E., Vago, R., Sanchez, A. M., Podini, P., Zarovni, N., Murdica, V., Rizzo, R., Bortolotti, D., Candiani, M., & Viganò, P. (2017). Secretome of in vitro cultured human embryos contains extracellular vesicles that are uptaken by the maternal side. *Scientific Reports*, *7*(1). https://doi.org/10.1038/s41598-017-05549-w

Giuliano, R., Maione, A., Vallefuoco, A., Sorrentino, U., & Zuccarello, D. (2023). Preimplantation Genetic Testing for Genetic Diseases: Limits and Review of Current Literature. In *Genes* (Vol. 14, Issue 11). Multidisciplinary Digital Publishing Institute (MDPI). https://doi.org/10.3390/genes14112095

Hambiliki, F., Ström, S., Zhang, P., & Stavreus-Evers, A. (2012). Co-localization of NANOG and OCT4 in human pre-implantation embryos and in human embryonic stem cells. *Journal of Assisted Reproduction and Genetics*, *29*(10), 1021–1028. https://doi.org/10.1007/s10815-012-9824-9

Handyside, A. H., Kontogianni, E. H., Hardy, k., & Winston, R. M. L. (1990). Pregnancies from biopsied human preimplantation embryos sexed by Y-specific DNA amplification. *Nature*, *344*, 768–770.

Hawke, D. C., Watson, A. J., & Betts, D. H. (2021). Extracellular vesicles, microRNA and the preimplantation embryo: non-invasive clues of embryo well-being. *Reproductive BioMedicine Online*, *42*, 39–54. https://doi.org/10.1016/j

Hurtado de Mendoza, M. V., Ten, J., Arroyo, G., de los Santos, M. J., Pons, M. C., Cuadros, J., Prados, F., González, B., de Mendoza, M. V. H., de los Santos, M. J., Mugica, A., Vilches, M. Á., & et al. (2015). CUADERNOS DE EMBRIOLOGÍA CLÍNICA. In *ASEBIR : Vol. 3ª Edición* (pp. 1–98). www.gobalo.es

Jankovičová, J., Neuerová, Z., Sečová, P., Bartóková, M., Bubeníčková, F., Komrsková, K., Postlerová, P., & Antalíková, J. (2020). Tetraspanins in mammalian reproduction: spermatozoa, oocytes and embryos. In *Medical Microbiology and Immunology* (Vol. 209, Issue 4, pp. 407–425). Springer. https://doi.org/10.1007/s00430-020-00676-0

Jankovičová, J., Sečová, P., Michalková, K., & Antalíková, J. (2020). Tetraspanins, more than markers of extracellular vesicles in reproduction. In *International Journal of Molecular Sciences* (Vol. 21, Issue 20, pp. 1–30). MDPI AG. https://doi.org/10.3390/ijms21207568

Kalluri, R., & LeBleu, V. S. (2020). The biology, function, and biomedical applications of exosomes. In *Science* (Vol. 367, Issue 6478). American Association for the Advancement of Science. https://doi.org/10.1126/science.aau6977

Karam, J., Méresse, S., Kremer, L., & Daher, W. (2020). The roles of tetraspanins in bacterial infections. In *Cellular Microbiology* (Vol. 22, Issue 12). Blackwell Publishing Ltd. https://doi.org/10.1111/cmi.13260

Kazuhiro Takeuchi. (2020). Pre-implantation genetic testing: Past, present, future. *Reproductive Medicine and Biology*, 27–40. https://doi.org/10.1111/rmb2.12352

Kokkali, G., Coticchio, G., Bronet, F., Celebi, C., Cimadomo, D., Goossens, V., Liss, J., Nunes, S., Sfontouris, I., Vermeulen, N., Zakharova, E., & De Rycke, M. (2020). ESHRE PGT Consortium and SIG Embryology good practice recommendations for polar body and embryo biopsy for PGT. *Human Reproduction Open*, *2020*(3). https://doi.org/10.1093/hropen/hoaa020

Kotze, D., Kruger, T. F., Lombard, C., Padayachee, T., Keskintepe, L., & Sher, G. (2013). The effect of the biochemical marker soluble human leukocyte antigen G on pregnancy outcome in assisted reproductive technology - A multicenter study. *Fertility and Sterility*, *100*(5), 1303–1309. https://doi.org/10.1016/j.fertnstert.2013.07.1977

Kowalczyk, A., Wrzecińska, M., Czerniawska-Piątkowska, E., & Kupczyński, R. (2022). Exosomes – Spectacular role in reproduction. In *Biomedicine and Pharmacotherapy* (Vol. 148). Elsevier Masson s.r.l. https://doi.org/10.1016/j.biopha.2022.112752

Kummer, D., Steinbacher, T., Schwietzer, M. F., Thölmann, S., & Ebnet, K. (2020). Tetraspanins: integrating cell surface receptors to functional microdomains in homeostasis and disease. In *Medical Microbiology and Immunology* (Vol. 209, Issue 4, pp. 397–405). Springer. https://doi.org/10.1007/s00430-020-00673-3

Lee, M., Oh, J. N., Choe, G. C., Choi, K. H., Lee, D. K., Kim, S. H., Jeong, J., Ahn, Y., & Lee, C. K. (2023). NANOG expression in parthenogenetic porcine blastocysts is required for intact lineage specification and pluripotency. *Animal Bioscience*, *36*(12), 1905–1917. https://doi.org/10.5713/ab.23.0210

Levy, R., Benchaib, M., Cordonier, H., Souchier, C., & Guerin, J. F. (1998). Annexin V labelling and terminal transferase-mediated DNA end labelling (TUNEL) assay in human arrested embryos. In *Molecular Human Reproduction* (Vol. 4, Issue 8).

Li, N., Guan, Y., Ren, B., Zhang, Y., Du, Y., Kong, H., Zhang, Y., & Lou, H. (2022). Effect of Blastocyst Morphology and Developmental Rate on Euploidy and Live Birth Rates in Preimplantation Genetic Testing for Aneuploidy Cycles With Single-Embryo Transfer. *Frontiers in Endocrinology*, *13*. https://doi.org/10.3389/fendo.2022.858042

Liu, W. M., Cao, Y. J., Yang, Y. J., Li, J., Hu, Z., & Duan, E. K. (2006). Tetraspanin CD9 regulates invasion during mouse embryo implantation. *Journal of Molecular Endocrinology*, *36*(1), 121–130. https://doi.org/10.1677/jme.1.01910

Malmsten, J., Zaninovic, N., Zhan, Q., Toschi, M., Rosenwaks, Z., Shan, J., Shear, M., Vaughan, D., Modest, A., Murphy, L., Seidler, E., Hacker, M., Sakkas, D., Penzias, A. S., Ermisch, A. F., Logsdon, D. M., Schlenker, T. W., Hamm, J. M., McCormick, S., … Krisher, R. L. (2018). Blastocysts cryopreserved on day 5 have higher live birth rates than those cryopreserved on day 6 in frozen embryo transfer (FET) cycles. *AM Human Reproduction*, *6*(3), 30. https://doi.org/10.1093/humrep/dey00

Martín, Á., Mercader, A., Beltrán, D., Mifsud, A., Nohales, M., Pardiñas, M. L., Ortega-Jaén, D., & de los Santos, M. J. (2024). Trophectoderm cells of human mosaic embryos display increased apoptotic levels and impaired differentiation capacity: a molecular clue regarding their reproductive fate? *Human Reproduction*, *39*(4), 709–723. https://doi.org/10.1093/humrep/deae009

Mitsui, K., Tokuzawa, Y., Itoh, H., Segawa, K., Murakami, M., Takahashi, K., Maruyama, M., Maeda, M., & Yamanaka, S. (2003). *The Homeoprotein Nanog Is Required for Maintenance of Pluripotency in Mouse Epiblast and ES Cells*. http://www.ncbi.nlm.nih.gov/UniGene/

Ng, Y. H., Rome, S., Jalabert, A., Forterre, A., Singh, H., Hincks, C. L., & Salamonsen, L. A. (2013). Endometrial Exosomes/Microvesicles in the Uterine Microenvironment: A New Paradigm for Embryo-Endometrial Cross Talk at Implantation. *PLoS ONE*, *8*(3). https://doi.org/10.1371/journal.pone.0058502

Niu, Z., Wang, L., Pang, R. T. K., Guo, Y., Yeung, W. S. B., & Yao, Y. (2017). A meta-analysis of the impact of human leukocyte antigen-G on the outcomes of IVF/ICSI. *Reproductive BioMedicine Online*, *34*(6), 611–618. https://doi.org/10.1016/j.rbmo.2017.03.002

Pallinger, E., Bognar, Z., Bodis, J., Csabai, T., Farkas, N., Godony, K., Varnagy, A., Buzas, E., & Szekeres-Bartho, J. (2017). A simple and rapid flow cytometry-based assay to identify a competent embryo prior to embryo transfer. *Scientific Reports*, *7*. https://doi.org/10.1038/srep39927

Papadopoulou, M. I., Papatheodorou, A., Vorniotaki, A., Christoforidis, N., & Chatziparasidou, A. (2021). *P-224 Multinucleated and non-multinucleated embryos in PGT-A cycles: Is there any difference?*

Parikh, F. R., Athalye, A. S., Naik, N. J., Naik, D. J., Sanap, R. R., & Madon, P. F. (2018). Preimplantation genetic testing: Its evolution, where are we today? In *Journal of Human Reproductive Sciences* (Vol. 11, Issue 4, pp. 306–314). Wolters Kluwer Medknow Publications. https://doi.org/10.4103/jhrs.JHRS_132_18

Radwan, P., Tarnowska, A., Piekarska, K., Wiśniewski, A., Krasiński, R., Radwan, M., & Nowak, I. (2022). The impact of soluble HLA-G in IVF/ICSI embryo culture medium on

implantation success. *Frontiers in Immunology*, *13*. https://doi.org/10.3389/fimmu.2022.982518

Ramos-Ibeas, P., Gimeno, I., Cañón-Beltrán, K., Gutiérrez-Adán, A., Rizos, D., & Gómez, E. (2020). Senescence and Apoptosis During in vitro Embryo Development in a Bovine Model. In *Frontiers in Cell and Developmental Biology* (Vol. 8). Frontiers Media S.A. https://doi.org/10.3389/fcell.2020.619902

Roussev, R. G., & Coulam, C. B. (2007). HLA-G and its role in implantation (review). In *Journal of Assisted Reproduction and Genetics* (Vol. 24, Issue 7, pp. 288–295). https://doi.org/10.1007/s10815-007-9148-3

Shahbazi, M. N., Wang, T., Tao, X., Weatherbee, B. A. T., Sun, L., Zhan, Y., Keller, L., Smith, G. D., Pellicer, A., Scott, R. T., Seli, E., & Zernicka-Goetz, M. (2020). Developmental potential of aneuploid human embryos cultured beyond implantation. *Nature Communications*, *11*(1). https://doi.org/10.1038/s41467-020-17764-7

Shen, L., Diao, Z., Sun, H. X., Yan, G. J., Wang, Z., Li, R. T., Dai, Y., Wang, J., Li, J., Ding, H., Zhao, G., Zheng, M., Xue, P., Liu, M., Zhou, Y., & Hu, Y. (2017). Up-regulation of CD81 inhibits cytotrophoblast invasion and mediates maternal endothelial cell dysfunction in preeclampsia. *Proceedings of the National Academy of Sciences of the United States of America*, *114*(8), 1940–1945. https://doi.org/10.1073/pnas.1617601114

Silva, J., Nichols, J., Theunissen, T. W., Guo, G., van Oosten, A. L., Barrandon, O., Wray, J., Yamanaka, S., Chambers, I., & Smith, A. (2009). Nanog Is the Gateway to the Pluripotent Ground State. *Cell*, *138*(4), 722–737. https://doi.org/10.1016/j.cell.2009.07.039

Sordia-Hernandez, L. H., Morales-Martinez, F. A., González-Colmenero, F. D., Flores-Rodriguez, A., Leyva-Camacho, P. C., Sordia-Piñeyro, M. O., Valdés-Martínez, O. H., García-Luna, S. M., Rodríguez-Guajardo, R., & Sordia-Piñeyro, L. H. (2022). The Effects of Preimplantation Genetic Testing for Aneuploidy (PGT-A) on Patient-Important Outcomes in Embryo Transfer Cases: A Meta-Analysis. *Journal of Reproduction and Infertility*, *23*(4), 231–249. https://doi.org/10.18502/jri.v23i4.10808

Talbot, A. L., Alexopoulou, E., Kallemose, T., Freiesleben, N. L. C., Nielsen, H. S., & Zedeler, A. (2022). Binucleated embryos at the two-cell stage show higher blastocyst formation rates and higher pregnancy and live birth rates compared to non-multinucleated embryos. *Human Reproduction Open*, *2022*(4). https://doi.org/10.1093/hropen/hoac049

Taylor, T. H., Gitlin, S. A., Patrick, J. L., Crain, J. L., Wilson, J. M., & Griffin, D. K. (2014). The origin, mechanisms, incidence and clinical consequences of chromosomal mosaicism in humans. *Human Reproduction Update*, *20*(4), 571–581. https://doi.org/10.1093/humupd/dmu016

Tenchov, R. (2022, December 2). *La evolución del exosoma: de actor marginal a estrella en alza*. American Chemical Society, (Https://Www.Cas.Org/Es-Es/Resources/Cas-Insights/Biotechnology/Evolving-Exosome-Small-Player-Rising-Star).

Termini, C. M., & Gillette, J. M. (2017). Tetraspanins function as regulators of cellular signaling. In *Frontiers in Cell and Developmental Biology* (Vol. 5, Issue APR). Frontiers Media S.A. https://doi.org/10.3389/fcell.2017.00034

Tomic, M., Vrtacnik Bokal, E., & Stimpfel, M. (2022). Non-Invasive Preimplantation Genetic Testing for Aneuploidy and the Mystery of Genetic Material: A Review Article. In *International Journal of Molecular Sciences* (Vol. 23, Issue 7). MDPI. https://doi.org/10.3390/ijms23073568

Toribio, V., & Yáñez-Mó, M. (2022). Tetraspanins interweave EV secretion, endosomal network dynamics and cellular metabolism. *European Journal of Cell Biology*, *101*(3). https://doi.org/10.1016/j.ejcb.2022.151229

Van Niel, G., D'Angelo, G., & Raposo, G. (2018). Shedding light on the cell biology of extracellular vesicles. In *Nature Reviews Molecular Cell Biology* (Vol. 19, Issue 4, pp. 213–228). Nature Publishing Group. https://doi.org/10.1038/nrm.2017.125

Vera-Rodriguez, M., Diez-Juan, A., Jimenez-Almazan, J., Martinez, S., Navarro, R., Peinado, V., Mercader, A., Meseguer, M., Blesa, D., Moreno, I., Valbuena, D., Rubio, C., & Simon, C. (2018). Origin and composition of cell-free DNA in spent medium from human embryo culture during preimplantation development. *Human Reproduction*, *33*(4), 745–756. https://doi.org/10.1093/humrep/dey028

Vermes, I., Haanen, C., Steffens-Nakken, H., & Reutelingsperger, C. (1995). A novel assay for apoptosis Flow cytometric detection of phosphatidylserine early apoptotic cells using fluorescein labelled expression on Annexin V. In *JOURNAL OF MMMO~OGICAL ELSEVTER Journal of Immunological Methods* (Vol. 184).

Viotti, M. (2020). Preimplantation genetic testing for chromosomal abnormalities: Aneuploidy, mosaicism, and structural rearrangements. In *Genes* (Vol. 11, Issue 6). MDPI AG. https://doi.org/10.3390/genes11060602

Vyas, P., Balakier, H., & Librach, C. L. (2019). Ultrastructural identification of CD9 positive extracellular vesicles released from human embryos and transported through the zona pellucida. *Systems Biology in Reproductive Medicine*, *65*(4), 273–280. https://doi.org/10.1080/19396368.2019.1619858

Wang, J. M., Zhao, H. X., Wang, L., Gao, Z. Y., & Yao, Y. Q. (2013). The human leukocyte antigen G promotes trophoblast fusion and β-hCG production through the Erk1/2 pathway in human choriocarcinoma cell lines. *Biochemical and Biophysical Research Communications*, *434*(3), 460–465. https://doi.org/10.1016/j.bbrc.2013.04.004

Wells, D. (2014). Next-generation sequencing: The dawn of a new era for preimplantation genetic diagnostics. In *Fertility and Sterility* (Vol. 101, Issue 5, pp. 1250–1251). Elsevier Inc. https://doi.org/10.1016/j.fertnstert.2014.03.006

Willms, E., Cabañas, C., Mäger, I., Wood, M. J. A., & Vader, P. (2018). Extracellular vesicle heterogeneity: Subpopulations, isolation techniques, and diverse functions in cancer progression. In *Frontiers in Immunology* (Vol. 9, Issue APR). Frontiers Media S.A. https://doi.org/10.3389/fimmu.2018.00738

Yee, C. S., & Tian, T. S. (2019). Choosing between Day 5 and Day 6 blastocyst: Comparison of aneuploidy rates and pregnancy rates. *Reproductive BioMedicine Online*, *38*, e31. https://doi.org/10.1016/j.rbmo.2019.03.051

Zaborowski, M. P., Balaj, L., Breakefield, X. O., & Lai, C. P. (2015). Extracellular Vesicles: Composition, Biological Relevance, and Methods of Study. In *BioScience* (Vol. 65, Issue 8, pp. 783–797). Oxford University Press. https://doi.org/10.1093/biosci/biv084

Zegers-Hochschild, F., Adamson, G. D., de Mouzon, J., Ishihara, O., Mansour, R., Nygren, K., Sullivan, E., & Vanderpoel, S. (2009). International Committee for Monitoring Assisted Reproductive Technology (ICMART) and the World Health Organization (WHO) revised glossary of ART terminology, 2009*. *Fertility and Sterility*, *92*(5), 1520–1524. https://doi.org/10.1016/j.fertnstert.2009.09.009

Zhang, W., Sui, Y., Ni, J., & Yang, T. (2016). Insights into the Nanog gene: A propeller for stemness in primitive stem cells. In *International Journal of Biological Sciences* (Vol. 12,

Issue 11, pp. 1372–1381). Ivyspring International Publisher. https://doi.org/10.7150/ijbs.16349

Zhou, W., Zhang, T., Lian, Y., & Zhang, W. (2022). Chapter 7 - Roles of Extracellular Vesicles in Human Reproduction. In *Extracellular Vesicles - Roles in Diaseases, Pathogenesis and Therapy*. https://doi.org/10.5772/intechopen.101046

7. Appendices

Supplementary Table 1 – Morphological characteristics, time of culture durations, and Preimplantation Genetic Testing (PGT) outcomes of embryos from Group 1 (pre-vitrification embryos). blastocyst (B); expanded (E); hatched (Hd); without information (-); nuclei (N).

G1	G2	Embryo Quality	Development Day	Time in Spent Medium	Multinucleation	Fragmentation	PGT Results
P2	**D123**	BEBB	5	00:45	2N	15%	Euploid
P3	**0**	BEBB	5	00:45	0	0	Euploid
P4	**0**	BEAB	5	00:45	0	15%	Mosaic
P5	**0**	BECB	5	00:53	0	20%	Euploid
P6	**0**	BEBB	5	00:19	0	15%	Euploid
P7	**D48**	BEAB	5	00:19	2N	20%	Euploid
P8	**0**	BHdBB	5	00:27	2N	0	Euploid
P9	**0**	BEBA	5	00:27	2N	0	Monosomy X
P10	**0**	BHdBB	6	00:21	0	30%	Trisomy 2
P11	**0**	BECC	6	00:33	0	25%	Trisomy 22
P12	**0**	BHdBB	6	00:33	3N	20%	Monosomy 16
P13	**0**	BEBB	5	00:29	2N	20%	Monosomy 2 + Trisomy 15
P14	**D49**	BTBB	5	00:29	0	15%	Euploid
P15	**0**	BEBC	5	00:29	0	25%	Euploid
P48	**0**	BEBC	6	-	0	0	Monosomy 7
P49	**0**	BHdBB	6	-	0	15%	Trisomy 21
P16	**0**	BHBB	5	01:20	0	0	Euploid
P17	**0**	BHAB	5	01:20	0	15%	Euploid
P18	**0**	BHdAB	5	00:40	3N	0	Trisomy 15
P19	**D75**	BHdAA	5	00:40	2N	0	Euploid
P20	**0**	BHdAA	5	00:41	0	30%	Trisomy 21
P21	**0**	BHdBA	5	00:41	3N	0	Monosomy 13
P22	**D65**	BHdBC	6	00:17	2N	30%	Euploid
P23	**D74**	BHdAB	5	00:06	0	0	Euploid
P24	**D83**	BEBB	5	00:17	0	0	Euploid
P25	**0**	BEBB	5	00:17	0	0	Monosomy 16 + Trisomy 13
P26	**0**	BEBB	5	00:23	3N	0	Monosomy 12
P27	**0**	BEBB	5	00:23	2N	0	Euploid
P28	**D82**	BEAB	5	00:15	0	0	Euploid
P29	**0**	BEAB	5	00:15	0	0	Euploid
P30	**0**	BEBB	5	00:17	4N	0	Monosomy 10
P31	**0**	BBC	6	00:52	2N	15%	Monosomy 15 and 18 + Trisomy 12 and 17
P32	**0**	BBB	5	00:38	2N	0	Monosomy 2
P33	**0**	BEBB	5	00:30	2N	0	Trisomy 22
P34	**0**	BEAB	5	00:30	0	0	Trisomy 21
P35	**0**	BHdBB	5	00:31	2N	0	Euploid
P36	**0**	BHdBB	5	00:34	2N	0	Euploid
P37	**0**	BECB	5	00:20	3N	0	Trisomy 22
P38	**0**	BEBB	5	00:20	0	0	Euploid
P39	**0**	BEBC	5	00:36	-	-	Trisomy 2, 12 e 22
P40	**0**	BEBB	5	00:36	-	-	Euploid
P41	**0**	BHdCB	6	00:17	-	-	Trisomy 12 e 21
P42	**0**	BEBB	5	00:15	3N and 4N	0	Monosomy 9 + Parcial Monosomy Xq21.2q28
P43	**0**	BEBC	5	00:15	4N	0	Monosomy 2
P44	**0**	BHdAA	5	00:31	0	0	-
P45	**0**	BECB	5	00:23	0	0	-
P46	**0**	BBB	5	00:23	0	15%	-
P47	**0**	BBB	5	00:20	0	15%	-

Supplementary Table 2 - Clinical characteristics and infertility history of patients from Group 1 (pre-vitrification embryos). This table identifies the type and duration of infertility, the number of previous assisted reproduction cycles, and the number and clinical indication for preimplantation genetic testing (PGT). Also details the number of previous embryo transfers, miscarriages, and live births for each patient. Additionally, includes the age and body mass index (BMI) of the patients, Anti-Müllerian Hormone (AMH) levels, semen analysis results, and reproductive diseases. In vitro fertilization (FIV); Artificial Insemination with Husband's Semen (AIH); advanced maternal age (AMA); severe male factor (SMF); recurrent miscarriages (RM); recurrent implantation failure (RIF); motile sperm count (REM); fragmentation index (FI); without information (-).

G1	G2	Esterility Type	Esterility Duration	Prev. Cicles	Prev. PGT	PGT Indic.	Prev. Transf.	Miscarriages	Child-Birth	Age ♀	Age ♂	BMI ♀	BMI ♂	AMH	Seminogram ♂	Diseases ♀	Diseases ♂
P2	D123	1	3 years	1 FIV	0	SMF	1	0	0	28	44	22,1	25,7	9,6	OligoAsthenoTeratozoospermia REM: 0,2M/mL FI: 37,9% - ZYMOT	0	Unilateral variocele and normal Y microdeleções
P3	0																
P4	0																
P5	0																
P6	0																
P7	D48																
P8	0																
P9	0																
P10	0																
P11	0	1	3 years	1 FIV	0	SMF	0	0	0	39	39	21,9	23,6	1,8	OligoAsthenoTeratozoospermia REM:0,8M/mL FI:33% - ZYMOT	0	0
P12	0																
P13	0	2	1,5 years	1 FIV	0	AMA	0	1	1	39	41	30,4	24,1	0,745	NORMOzoospermia REM: 23M/mL FI: 18%	0	0
P14	D49																
P15	0																
P48	0																
P49	0																
P16	0	2	-	0	0	RM	0	4	1	36	33	21,1	26,8	1,33	NORMOzoospermia REM:10M/mL FI:19,5%	0	0
P17	0																
P18	0	1	8 months	1 FIV	1	SMF	0	0	0	37	38	20,9	33,6	1,56	Oligoteratozoospermia REM:0,7milh/mL FI:25%	0	0
P19	D75																
P20	0																
P21	0																
P22	D65	1	1,5 years	1 FIV	0	AMA	0	0	0	42	41	21,8	28,2	0,42	Teratozoospermia REM:3M/mL FI:12.6%	2 subserous fibroids	0
P23	D74	1	8 years	0	0	SMF	0	0	0	36	37	18,4	25,2	2,26	OligoAsthenoTeratozoospermia REM:1milh/mL FI:26.5% - ZYMOT	0	XYY karyotype

P24	**D83**	1	1 year	1 FIV	1	AMA	1	0	0	41	42	20,1	-	4,11	NORMOzoospermia REM:18M/mL FI:8,4%	0	0
P25	**0**																
P26	**0**	2	1 year	1 FIV	1	RM	0	2		37	41	19,6	24,2	3,04	NORMOzoospermia REM:2M/mL FI:24%	0	0
P27	**0**																
P28	**D82**																
P29	**0**																
P30	**0**	-	-	1 FIV	1	SMF + AMA	1	0	1	43	42	22,8	24,9	2,99	NORMOzoospermia REM:26M/mL FI: 23%	0	Pericentric inversion of cr.12 (46,XY, inv(12) (p11.2q14) - PGT-SR
P31	**0**	1	1 year	0	0	AMA + RM	0	2	0	43	38	20,5	25,8	2,78	NORMOzoospermia REM:45M/mL FI:19,5% - ZYMOT	type 6 myoma and several subserous	0
P32	**0**	2	1 year	1 FIV	0	AMA	0	1	1	43	41	19,7	21,4	0,68	NORMOzoospermia REM:16M/mL FI:13%	0	left varicocele
P33	**0**	1	3 years	2 AIH	0	SMF	0	0	0	38	38	17,1	29,8	6,56	OligoAsthenozoospermia REM:1,5M/mL FI:20,5% - ZYMOT	0	0
P34	**0**																
P35	**0**																
P36	**0**																
P37	**0**																
P38	**0**																
P39	**0**																
P40	**0**																
P41	**0**																
P42	**0**	1	4 years	0	0	AMA	0	1 BQ	0	42	51	17,6	24,2	-	NORMOzoospermia REM:28M/mL FI:19,3%	0	0
P43	**0**																
P44	**D121**	1	2 years	3 AIH	0	SMF	0	0	0	38	41	23,3	24,2	1,54	NORMOzoospermia REM:21M/mL FI: 19,9%	0	47XXY/46XY mosaicism - PGT-SR
P45	**0**	1	1,5 years	2 FIV	0	AMA	2	1 BQ	0	40	37	20	24,8	1,61	NORMOzoospermia REM:20M/mL FI:16%	0	0
P46	**0**																
P47	**0**	1	1 year	4 FIV	1	RIF + AMA	4	1	1	41	40	20,8	24,3	0,641	AsthenoTeratozoospermia REM:3M/mL FI:34% ZYMOT	0	0

Supplementary Table 3 - Morphological characteristics, time of culture durations, and Preimplantation Genetic Testing (PGT) outcomes of embryos from Group2 (post-devitrification embryos). blastocyst (B); expanded (E); hatched (Hd); without information (-); nuclei (N).

G2	G1	Embryo Quality	Development Day	Multinucleation	Fragmentation	PGT Results	Time in Spent Medium	Age ♀ Transf.	Endometrium	E2	P4	Pregnancy Result
D4	0	BBB	5	-	-	Euploid	02:30	39	9	213	10,91	Yes
D5	0	BHdCB	6	-	-	Euploid	02:30	36	13	118	22,72	No
D17	0	BECB	6	-	-	Euploid	02:30	37	10	300	15,28	No
D19	0	BBB	6	-	-	Euploid	02:30	37	12	79	21,85	Yes
D31	0	BHdAA	5	0	15%	Euploid	02:30	35	10	88,7	32,6	No
D34	0	BEAA	5	0	15%	Euploid	02:30	35	8	136	20,35	Yes
D35	0	BHdAB	5	2N	0	Euploid	02:00	36	8,8	172,2	26,87	Yes
D37	0	BEAB	5	0	0	Euploid	02:15	41	7,5	208	7,62	Yes
D39	0	BEBB	5	2N	0	Euploid	02:00	48	9	1067	13,27	Yes
D47	0	BBC	5	-	-	Euploid	03:00	38	12	126	24,4	Yes
D48	P7	BEAB	5	2N	20%	Euploid	02:30	28	11	126	20,16	Yes
D49	P14	BTBB	5	0	15%	Euploid	02:30	40	16	526	28,52	Yes
D52	0	BEBC	5	-	-	Euploid	02:15	44	10,5	130	30,62	Yes
D65	P22	BHdBC	6	2N	30%	Euploid	02:00	43	11	148	28,19	No
D67	0	BEBB	5	0	0	Euploid	02:00	44	11,3	159	8,51	No
D70	0	BEBB	5	0	0	Euploid	02:00	30	9,9	174	11,41	Yes
D72	0	BECB	5	-	-	Euploid	02:30	40	8,8	210	23,77	Yes
D74	P23	BHdAB	5	0	0	Euploid	02:30	36	9,5	148,7	31,8	Yes
D75	P19	BHdAA	5	2N	0	Euploid	02:30	37	10	110	29,3	No
D81	0	BEAA	5	0	15%	Euploid	02:30	35	-	82,35	30,75	Yes
D82	P28	BEAB	5	0	0	Euploid	02:30	37	9,5	269	16,79	No
D83	P24	BEBB	5	0	0	Euploid	02:30	41	9,6	205	16,47	Yes
D88	0	BEAA	5	0	15%	Euploid	02:30	39	9	198	26,77	Yes
D93	0	BHdBA	5	-	-	Euploid	02:00	39	8	88	9,52	Yes
D96	0	BHdBB	6	0	0	Euploid	02:00	38	8,2	70	33,69	Yes
D104	0	BHdCB	6	-	-	Euploid	02:00	36	13,3	899	14,11	Yes
D106	0	BHdAB	5	-	-	Euploid	02:00	40	7	144	24,8	No
D110	0	BEAB	5	-	-	Euploid	02:30	36	9,5	104	29,1	Yes
D111	0	BEBB	5	-	-	Euploid	02:00	39	11	382	17,34	Yes
D120	0	BHdCB	6	-	-	Euploid	02:00	30	9	193	9,88	-
D121	P44	BHdAA	5	-	-	Euploid	02:00	39	12,1	248	12,61	-
D123	P2	BEBB	5	-	-	Euploid	02:00	29	-	103,8	23,84	-

Supplementary Table 4 - Clinical characteristics and infertility history of patients from Group 2 (post-devitrification embryos). This table identifies the type and duration of infertility, the number of previous assisted reproduction cycles, and the number and clinical indication for preimplantation genetic testing (PGT). Also details the number of previous embryo transfers, miscarriages, and live births for each patient. Additionally, includes the age and body mass index (BMI) of the patients, Anti-Müllerian Hormone (AMH) levels, semen analysis results, and reproductive diseases. In vitro fertilization (FIV); Artificial Insemination with Husband's Semen (AIH); Ectopic Pregnancy (EP); Chemical Pregnancy (CP); advanced maternal age (AMA); severe male factor (SMF); recurrent miscarriages (RM); recurrent implantation failure (RIF); motile sperm count (REM); fragmentation index (FI); without information (-).

G2	G1	Esterility Type	Esterility Duration	Prev. Cicles	Prev. PGT	PGT Ind.	Previous Transf.	Miscarriages	Child-Birth	Age ♀ FIV	Age ♂ FIV	BMI ♀	BMI ♂	AMH	Seminogram ♂	Diseases ♀	Diseases ♂
D4	0	1	-	0	0	RM	1 FIV	3 + 3 CP + 2 EP	0	38	35	27,7	-	2,64	NORMOzoospermia REM:13M/mL FI: 11,6%	0	0
D5	0	1	-	2	0	RM	3 FIV	1 + 3 EP	0	35	33	24,7	24,5	0,8	NORMOzoospermia REM:20M/mL FI: 22,6%	Salpinguectomia bilateral	0
D17	0	1	5 years	1	0	RM	4 FIV	1 + 1 CP	0	43	46	18,2	24,5	3,39	NORMOzoospermia REM:11M/mL FI: 14,4%	0	0
D19	0	1	1,5 years	0	1	RIF	2 FIV	-	0	36	35	20,9	27,5	-	NORMOzoospermia REM:6M/mL FI:20,9%	0	0
D31	0	1	years	0	0	SMF	0	1	0	35	35	21,5	25	1,25	Teratozoospermia REM:7M/mL FI:14%	0	0
D34	0	-	-	0	0	RM	-	2	0	35	38	23,7	25,4	4,2	NORMOzoospermia REM:25M/mL FI: 21,7%	Hereditary Angioedema	0
D35	0	-	-	0	0	RM	0	1	0	35	30	22,3	23,4	0,8	NORMOzoospermia REM:18M/mL FI: 8%	0	Epidermolisis bullosa (HAD) and Cystic Fibrosis (Delta F508)
D37	0	-	-	0	0	AMA	0	0	0	41	-	? 62Kg (20)	-	1,82	NORMOzoospermia_Donor	Hidrossalpinx and 1 polyp	0
D39	0	1	8 months	1	0	AMA	0	0	0	40	42	20,9	26,9	0,36	Normozoospermia Hypospermia REM:8M/mL FI:17,2%	0	0
D47	0	2	1 year	0	0	AMA	0	0	1	38	39	25,1	27,4	3,5	NORMOzoospermia REM:9M/mL FI:20,5%	0	0
D48	P7	1	3 years	1	0	SMF	1 FIV	0	0	28	44	22,1	26	9,6	OligoAsthenoTeratozoospermia REM: 0,2 M/mL FI:	0	Unilateral variocele and

															37,9% ZYMOT		normal Y microdeletions
D49	P14	2	1,5 yeras	1	0	AMA	0	1	1	39	41	30,4	24,1	0,745	NORMOzoospermia REM:23M/mL FI: 18%	0	0
D52	0	2	-	1	0	RIF	3 FIV	1	2	42	38	23	23,9	3,9	NORMOzoospermia REM:12M/mL FI:10,4%	0	0
D65	P22	1	1,5 years	1	0	IMA	0	0	0	42	41	21,8	28,2	0,42	Teratozoospermia REM:3mil/mL FI:12.6%	2 subserous fibroids	0
D67	0	-	-	1	1	IMA	1	0	1	42	42	24,9	23,1	1,25	NORMOzoospermia_ Donor	0	0
D70	0	1	2 years	0	0	RM	0	2 + 1 CP	0	30	30	-	-	1,79	NORMOzoospermia REM:28M/mL FI:5,4%	0	0
D72	0	1	2 years	0	3	SMF + RIF	2	1	0	22 Donor	37	20,5	30,4	2,1	OligoAsthenoTeratozoospermia REM:0,01M/mL FI:69,6%	0	0
D74	P23	1	8 months	0	0	SMF	0	0	0	36	37	18,4	25,2	2,26	OligoAsthenoTeratozoospermia REM:1milh/mL FI:26.5% ZYMOT	0	XYY karyotype
D75	P19	1	8 months	1	1	SMF	0	0	0	37	38	20,9	33,6	1,56	OligoTeratozoospermia REM:0,7milh/mL FI:25%	0	0
D81	0	1	1 year	0	1	RM	1	1	0	35	35	21,5	25	-	Teratozoospermia REM:7M/mL FI:14%	0	0
D82	P28	2	1 year	1	1	RM	0	1	1	37	41	19,6	24,2	3,04	NORMOzoospermia REM:2M/mL FI:24%	0	0
D83	P24	1	1 year	1	1	AMA	1	0	0	41	42	20,1	-	4,11	NORMOzoospermia REM:18M/Ml FI:8,4%	0	0
D88	0	1	1 year	0	0	AMA	0	0	0	39	44	22,5	25	9,38	NORMOzoospermia REM:9M/mL FI:15%	uterine myoma	Ulcerative colitis
D93	0	1	4 years	3	2	RM + RIF	5 FIV	5	0	37	36	-	-	3,58	Astenozoospermia REM:0,8M/mL FI:26%	0	0
D96	0	1	7 months	2	2	AMA	2 FIV	1	0	38	Donor	18,7	22,89	1,05	NORMOzoospermia_Donor	0	0
D104	0	1	2 years	0	0	RM	0	1	0	36	36	25,6	24,7	2,21	NORMOzoospermia REM:35M/mL FI:13%	0	0
D106	0	2	1 year	0	0	AMA	0	2	1	40	41	18,4	31,4	1,46	NORMOzoospermia REM:13M/mL FI:14,3%	0	0
D110	0	1	4 years	2	0	RIF	2 AIH	0	0	36	32	23,4	26,4	3,95	NORMOzoospermia REM:14M/mL FI:10,1%	0	0

D111	0	1	2 years	0	0	SMF	0	0	0	39	37	22,6	22,2	1,21	OligoAstenoTeratozoospermia REM:0,1M/mL FI:42%	0	0
D120	0	1	5 years	1	0	RIF	2 FIV + 3 AIH	1	0	30	33	25,3	30,7	1,88	NORMOzoospermia REM:15M/mL FI:21,8%	0	0
D121	P44	1	2 years	0	0	SMF	3 AIH	0	0	38	41	23,3	24,2	1,54	Normozoospermia REM:21M/mL FI:19,9%	0	47XXY/46XY mosaicism
D123	P2	1	3 years	1	0	SMF	1	1	0	28	44	22,1	26	9,6	OligoAstenoTeratozoospermia REM: 0,2 M/mL FI: 37,9% ZYMOT	0	Unilateral variocele and normal Y microdeletions

Supplementary Table 5 - Exossome Tetraspanin detailed analysis in the spent medium of Group 1 (pre-vitrification embryos).

G1	CD9 Channel	CD9	CD9 and CD63	CD9 and CD81	CD9, CD63 and CD81	CD63 Channel	CD63	CD63 and CD9	CD63 and CD81	CD63, CD9 and CD81	CD81 Channel	CD81	CD81 and CD9	CD81 and CD63	CD81, CD9 and CD63	MIgG1
P7	453	47	32	371	3	767	248	33	485	1	141	94	27	19	1	170
P11	118	26	28	64	0	318	183	39	95	1	55	26	15	15	0	60
P12	247	64	35	147	1	524	252	87	184	1	155	92	34	28	1	180
P14	127	38	34	53	1	372	259	30	83	0	83	39	18	25	1	90
P17	188	48	32	105	3	469	217	85	166	1	126	71	26	26	3	110
P18	201	49	32	119	2	584	255	102	225	2	209	130	53	25	1	150
P19	102	27	28	47	0	353	223	39	91	1	112	55	25	31	1	110
P21	183	47	0	133	3	323	139	46	136	1	70	52	16	1	1	100
P22	133	41	28	62	2	371	229	35	107	1	84	42	22	19	1	160
P23	159	37	44	77	1	433	217	64	152	1	127	64	30	32	1	120
P24	131	43	16	70	2	447	282	38	125	2	108	61	28	15	4	110
P26	89	28	14	46	0	428	207	59	161	1	114	73	27	14	0	110
P28	289	81	36	172	1	569	221	110	237	1	163	113	29	20	0	250
P30	160	45	19	95	0	444	219	75	148	1	135	83	30	21	1	150
P31	154	51	37	64	2	463	327	42	93	2	109	48	28	31	3	120
P35	230	71	41	64	0	317	54	103	160	1	124	68	23	32	1	110
P37	66	64	1	2	0	95	1	92	0	2	48	1	46	0	1	60
P41	150	40	30	81	0	195	44	43	108	0	100	59	17	24	0	110
P42	60	59	0	1	0	70	0	68	0	1	36	0	35	0	0	60
P43	253	221	19	8	5	152	5	143	4	0	95	1	78	5	11	100
P44	310	150	30	129	1	788	178	400	206	3	206	83	90	32	2	210
P48	143	42	33	68	1	357	191	45	120	1	101	60	18	22	1	120
P49	185	52	42	89	3	453	224	74	154	1	128	71	30	25	2	120

Supplementary Table 6 - Exossome Tetraspanin detailed analysis in the spent medium of Group 2 (post-devitrification embryos).

G2	CD9 Channel	CD9	CD9 and CD63	CD9 and CD81	CD9, CD63 and CD81	CD63 Channel	CD63	CD63 and CD9	CD63 and CD81	CD63, CD9 and CD81	CD81 Channel	CD81	CD81 and CD9	CD81 and CD63	CD81, CD9 and CD63	MIgG1
Dp4	285	61	46	144	35	670	341	103	197	29	321	85	93	61	82	110
Dp5	226	60	42	123	2	551	243	117	187	3	175	91	41	41	2	130
Dp19	203	46	56	97	5	504	288	81	132	4	155	80	36	32	7	140
Dp31	190	39	56	94	1	375	170	78	126	2	136	75	28	32	1	120
Dp34	185	49	42	87	7	514	333	65	111	5	88	38	22	24	3	100
Dp35	115	28	26	60	1	565	282	101	180	2	167	82	47	35	3	150
Dp37	238	66	52	120	0	391	113	103	175	1	148	71	32	46	0	110
Dp39	245	73	47	119	6	447	213	82	149	3	190	91	47	47	5	250
Dp47	178	37	52	87	2	461	217	67	176	2	153	70	32	48	3	150
Dp48	158	37	50	67	4	411	230	36	141	4	121	53	26	35	7	140
Dp49	322	91	54	169	9	793	220	197	353	23	300	201	56	37	7	400
Dp52	506	192	57	256	1	882	176	354	349	3	309	167	107	33	2	280
Dp65	183	51	31	91	10	413	213	48	144	8	179	104	31	14	30	150
Dp67	323	75	45	201	2	731	160	146	419	6	276	182	54	37	3	250
Dp70	314	89	48	174	3	704	170	222	307	5	234	139	61	29	5	180
Dp72	280	79	37	159	4	558	205	135	215	2	175	92	50	30	3	150
Dp74	147	34	38	66	9	456	287	53	110	6	140	64	35	33	7	130
Dp75	173	39	39	94	0	429	198	78	151	2	150	86	31	32	1	120
Dp81	234	85	34	113	2	511	140	181	186	3	191	98	60	31	3	130
Dp82	241	57	38	144	2	435	149	82	204	1	173	110	36	25	2	250
Dp83	131	36	19	75	1	334	151	45	137	1	101	56	22	19	4	70
Dp120	320	118	47	146	9	643	220	186	227	10	203	97	62	34	11	220
Dp121	514	226	51	236	0	1049	173	502	368	7	347	174	138	33	1	280

Supplementary Table 7 - Exossome Nanog, HLA-G and Annexin-V detailed analysis in the spent medium of Group 1 (pre-vitrification embryos). Nanog (N); HLA-G (H); Annexinn-V (A).

G1	CD9 Channel	CD9 Nanog	CD9 HLA-G	CD9 Annexin-V	CD9 N+H	CD9 N+A	CD9 H+A	CD9 N+H+A	CD63 Channel	CD63 Nanog	CD63 HLA-G	CD63 Annexin-V	CD63 N+H	CD63 N+A	CD63 H+A	CD63 N+H+A
P7	499	361	88	43	1	6	0	0	578	374	140	57	1	6	1	1
P12	510	322	121	60	1	5	1	1	763	419	231	96	3	7	1	5
P18	355	199	99	45	2	5	2	3	777	366	267	132	5	5	0	2
P21	522	327	102	78	2	10	3	1	689	424	164	87	2	8	2	2
P22	350	214	78	49	1	5	2	1	694	358	128	106	10	17	40	34
P24	453	303	82	57	1	6	2	3	570	374	122	65	1	7	0	0
P26	432	264	98	58	2	9	1	1	675	382	174	102	2	8	4	3
P28	495	316	94	75	0	7	1	1	666	388	158	107	1	7	3	2
P30	440	285	84	66	0	4	0	0	637	376	150	101	1	6	1	1
P37	948	259	611	63	7	4	1	3	836	513	196	114	1	10	1	1
P42	350	176	106	62	1	3	1	0	439	220	116	98	0	5	0	0
P43	430	242	98	72	1	8	7	2	626	300	167	147	2	7	1	1

G1	CD81 Channel	CD81 Nanog	CD81 HLA-G	CD81 Annexin-V	CD81 N+H	CD81 N+A	CD81 H+A	CD81 N+H+A	MIgG1
P7	402	282	72	43	0	4	0	1	300
P12	521	370	77	64	1	8	1	0	400
P18	459	314	70	62	0	6	5	1	440
P21	530	375	77	67	1	5	3	2	450
P22	366	246	61	52	0	4	1	1	320
P24	438	308	67	56	1	6	0	0	280
P26	389	283	44	54	1	7	1	0	400
P28	506	340	80	79	0	7	1	0	430
P30	516	305	116	82	1	8	2	1	380
P37	514	279	161	58	0	7	5	4	900

P42	364	197	103	59	1	4	0	0	250
P43	435	261	91	76	0	5	0	0	340

Supplementary Table 8 - Exossome Nanog, HLA-G and Annexin-V detailed analysis in the spent medium of Group 2 (post-devitrification embryos). Nanog (N); HLA-G (H); Annexinn-V (A).

G2	CD9 Channel	CD9 Nanog	CD9 HLA-G	CD9 Annexin-V	CD9 N+H	CD9 N+A	CD9 H+A	CD9 N+H+A	CD63 Channel	CD63 Nanog	CD63 HLA-G	CD63 Annexin-V	CD63 N+H	CD63 N+A	CD63 H+A	CD63 N+H+A
Dp4	521	205	246	62	3	3	1	1	646	254	261	72	5	3	1	2
Dp5	586	207	282	85	3	5	3	1	704	272	305	108	4	7	2	4
Dp47	320	216	52	46	1	5	0	0	403	278	71	45	2	7	0	0
Dp48	569	171	312	77	3	3	1	2	492	158	252	70	5	2	3	2
Dp52	621	167	364	78	4	2	2	4	749	207	436	93	5	3	2	3
Dp65	570	232	169	104	8	15	17	25	540	292	141	84	4	8	5	6
Dp82	431	276	86	60	0	6	3	1	531	324	107	88	2	8	1	1
Dp83	397	266	59	61	1	7	2	1	494	341	81	58	1	8	3	2

G2	CD81 Channel	CD81 Nanog	CD81 HLA-G	CD81 Annexin-V	CD81 N+H	CD81 N+A	CD81 H+A	CD81 N+H+A	MIgG1
Dp4	444	217	175	46	2	3	0	1	410
Dp5	397	167	165	58	2	1	1	1	440
Dp47	393	286	51	46	2	9	0	0	400
Dp48	466	167	243	50	3	1	1	1	300
Dp52	718	175	484	47	6	2	1	2	500
Dp65	318	213	59	41	0	4	0	0	330
Dp82	437	330	67	36	1	4	1	0	340
Dp83	382	279	51	47	0	4	0	1	360